APPLICATION OF RHEOLOGICAL ELEMENT METHOD (REM) MODEL FOR OPEN-PIT DESIGN OPTIMIZATION

by

Serata Geomechanics, Inc.
4124 Lakeside Drive
Richmond, California 94806

Work on this project was conducted under the auspices of the Department of Energy, Mines and Resources (Canada).

DSS FILE NUMBER: 09SQ.23440-7-9048

DSS CONTRACT NUMBER: 23440-7-9048/01-SQ

EMR SCIENTIFIC AUTHORITY: Dr. B. Manas Das

62 pp

17 March 1989

R-CM-89001

TABLE OF CONTENTS

1.0 INTRODUCTION 1

2.0 OBJECTIVES AND BENEFITS 1

3.0 METHOD OF STUDY 2

4.0 REM COMPUTER MODEL OF MINE GROUND 5

5.0 EVALUATION OF PIT DESIGNS 16

6.0 CONCLUSIONS 20

7.0 RECOMMENDATIONS 22

8.0 REFERENCES 23

APPENDICES

A SPDR Technology

B Numerical Results of REM Simulation

LIST OF TABLES

TABLE 1. Highwall Position from June 1987 to May 1988 6

TABLE 2. Excavation Stages in REM Model 7

TABLE 3. Preliminary Material Property Sets of REM Model 9

TABLE 4. Calibrated Material Property Sets of REM Model 11

TABLE 5. Movement at Elevation 530 meters (Estimated from Inclinometer Readings) 14

TABLE 6. Pit Design Variations for REM Simulation 17

TABLE 7. Maximum Values of Critical Parameters Predicted in REM Simulations 18

LIST OF FIGURES

following page

FIG. 1. REM constitutive model 4

FIG. 2. Geologic cross-section of Highvale Mine at Pit 03 . . . 5

FIG. 3. Finite element mesh of REM model 5

FIG. 4. Plan view of study site from June to September 1987 . . 15

FIG. 5. Cross-section through -3835 East, June to September 1987 15

FIG. 6. Plan view of study site from September to December 1987 15

FIG. 7. Cross-section through -3885 East, September to December 1987 15

FIG. 8. Positions of inclinometers in typical north-south profile 15

FIG. 9. Northward movement of stations S1 and S2 at Elevation 730 meters, with REM projection 15

FIG. 10. Northward movement of stations S3 and S4 at Elevation 730 meters, with REM projection 15

FIG. 11. Northward movement of stations S5 and S6 at Elevation 730 meters, with REM projection 15

FIG. 12. Material types and slope geometry parameters incorporated in REM model 17

1.0 INTRODUCTION

This report documents the computer simulation study performed by Serata Geomechanics, Inc. (SGI) of Richmond, California on behalf of the Department of Energy, Mines and Resources, Government of Canada (CANMET) in accordance with DSS Contract No. 23440-7-9048/01-SQ. The study was conducted at SGI's offices and laboratory from 1 November 1988 to 31 January 1989 by Mr. Chia-chi Chen, geotechnical engineer and Mr. Harish Goyal, project manager under the supervision of Dr. Shosei Serata.

The work reported herein focuses on field calibration of the site-specific computer model that was constructed for a certain area of Pit 03 of Highvale Mine under DSS Contract No. 23440-6-9021/01-SQ [1,2,3]. The recommendations presented in the previous work [3] are also reassessed utilizing the calibrated model. The model has been calibrated against ground deformation data collected in field monitoring programs conducted by the University of Alberta [4]. Three pit designs with different excavation geometries are evaluated by finite element computer simulation. The computer-projected results are examined and compared with those obtained in the previous project.

2.0 OBJECTIVES AND BENEFITS

Overall Objectives

The overall objectives of this study were:

- Calibration of the site-specific model developed under the previous contract [2,3]
- Application of the calibrated model to reassess the recommendations made earlier [3] regarding an optimum pit design for the particular area of Pit 03.

Specific Objectives

The specific objectives of the study were organized in three major tasks as follows:

- Task 1: Updating of site-specific model. A site-specific finite element model for REM® computer simulation, closely representing the geological and geomechanical conditions of the specific area of Pit 03 in Highvale Mine, had been constructed during the previous project. The material properties for the key strata and in situ stress state were determined through field and laboratory testing [1]. In this updating task, similar information for the strata not tested was obtained from SGI's data bank for best representation of the intact mine ground. Time-dependent mining activities under consideration were translated into sets of discrete external loading stages for representation in the computer simulation.

- Task 2: Model calibration. The preliminary model was calibrated against field measurement data provided by the University of Alberta. Calibration of the model was achieved through regression analysis by modifying material properties until a close match between computer-projected and field-measured ground deformation was obtained. External loading due to dragline weight was also incorporated in the model for calibration.

- Task 3: Design evaluation. To reassess the recommendations made earlier, we applied the calibrated model to simulate the performance of three pit designs with various slope geometries.

Benefits

The immediate benefit of the present study to TransAlta Utilities is the improvement of slope stability through REM design optimization. This advanced technology for evaluating slope stability in surface mining can be applied for optimization of Highvale Mine pit design to increase safety and

productivity. Further, the modeling capability of SGI's REM software is readily transferable to any other site in the region with slight modification of geologic and geomechanical conditions.

3.0 METHOD OF STUDY

Background

Despite recent advances in instrumentation and analysis techniques, typical practice in geomechanics employs little more than a set of empirical rules. To this extent, the study of geomechanics has yet to achieve the status of a fully quantitative science. This is particularly true with regard to the analysis, design, and construction of earth structures, especially in complex grounds. In order to overcome these limitations, SGI developed a new quantitative method of integrating field measurements and computer simulation analysis, which has proved effective in the design of underground structures. The method, termed the SPDR Technology®, comprises field instrumentation for measurement of the three basic ground conditions -- stress state (S), material properties (P), and ground deformation (D) -- and computer model analysis (R) for comprehension of the SPD field data. This approach enables the development of a site-specific computer model for the mine ground under consideration. The model is applied for quantitative comparison of candidate designs to identify the optimal mine configuration and excavation sequence with respect to safety and productivity.

SPDR Technology

The SPDR Technology may be expressed in its simplest form as follows:

$$S \cdot P \xrightarrow{R} D$$

This expression symbolizes that the stress state (S) present in a geologic formation interacts with the formation's material properties (P), producing deformation (D) of the ground. The overall mechanism of this process is simulated quantitatively by the REM computer program (R). The approach consists of systematically constructing a finite element computer model of the ground that matches the actual stress state and material properties of the ground, as measured in situ by sophisticated instrument probes. The differences found between the field-measured behavior and the idealized model are analyzed and then eliminated by modifying the base model until a close fit is achieved.

Development of the SPDR Technology proceeded as the relation R among S, P, and D behavior was established through field testing over a range of ground conditions. Application of the method has made the geomechanical work of analyzing, designing, and constructing earth structures in complex ground a truly quantitative effort. Appendix A provides a detailed description of the SPDR Technology.

REM Constitutive Model

The REM constitutive model enables comprehension of the time-dependent characteristics of earth materials. Fig. 1 depicts the REM model graphically as a mechanism of springs and dashpots. In the model, stress and strain are decomposed into two parts, viz., volumetric and deviatoric. Elastic and viscoelastic constitutive laws are applied to either of them. Additional viscoplastic constitutive equations introduced to the deviatoric portion play a significant role when the stress state of a solid exceeds a threshold value of octahedral shear strength (long-term creep strength). Several empirical functions are included in the model to simulate the effects on geologic materials of strength hardening with increased mean stress, deterioration for increasing shear strain, and temperature variation.

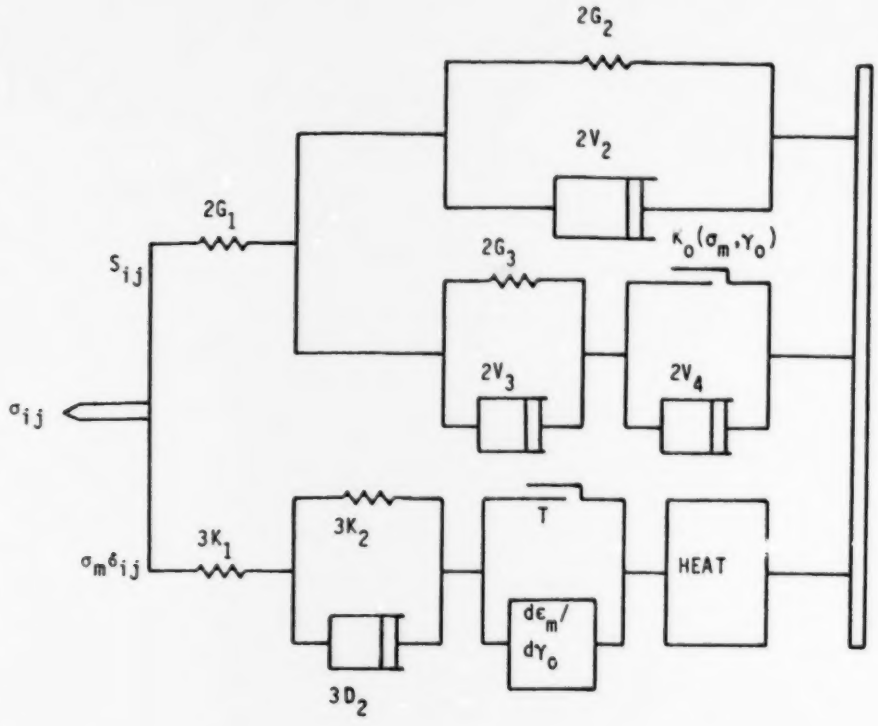

KEY

- σ_{ij}: Stress tensor
- ε_{ij}: Strain tensor
- τ_o : Shear stress
- γ_o : Shear strain
- σ_m : Hydrostatic stress
- ε_m : Hydrostatic strain

MATERIAL PROPERTY PARAMETERS

- G_1: Shear modulus
- G_2: Retarded shear modulus in viscoelastic state
- G_3: Retarded shear modulus in viscoplastic state
- V_2: Elastoviscosity in viscoelastic state
- V_3: Elastoviscosity in viscoplastic state
- V_4: Plastoviscosity in viscoplastic state
- K_o: Octahedral shear strength
- K_1: Bulk modulus
- K_2: Retarded bulk modulus in viscoelastic state
- D_2: Hydrostatic elastoviscosity in viscoelastic state
- T : Tensile strength

FIG. 1. REM constitutive model

4.0 REM COMPUTER MODEL OF MINE GROUND

Development of a successful REM computer model enables quantitative simulation of candidate mine designs to allow selection of an optimum design. The process of developing a site-specific computer model is an exacting and time-consuming effort: it involves integrating a large amount of data on material properties, in situ stress state, and ground deformation.

Model Development

Construction of the site-specific model for the Highvale Mine Pit 03 area included the following work:

- Geological and geometric representation. Six different geological strata -- till/displaced material, disturbed sandstone, displaced sandstone, shaley siltstone, bentonitic mudstone, and coal -- were identified in the Highvale Mine from the geologic cross-section shown in Fig. 2. Since the mine was excavated in one primary direction, use of a two-dimensional finite element mesh with the plane strain assumption was considered appropriate to represent the three-dimensional mine ground. The finite element mesh shown in Fig. 3 followed the actual excavation geometry of the mine ground as closely as possible. The mesh extends horizontally to a width of 1000 meters and vertically to a depth of 200 meters. In accordance with Table 1, which summarizes the highwall position (provided by the University of Alberta), the finite element mesh incorporated bank cut and chop cut angles of 45 degrees. The excavation angle of the coal seam was assigned as 80 degrees. The spoil piles had an angle of 30 degrees. These values represent the operational slope geometry for the Pit 03 study area.

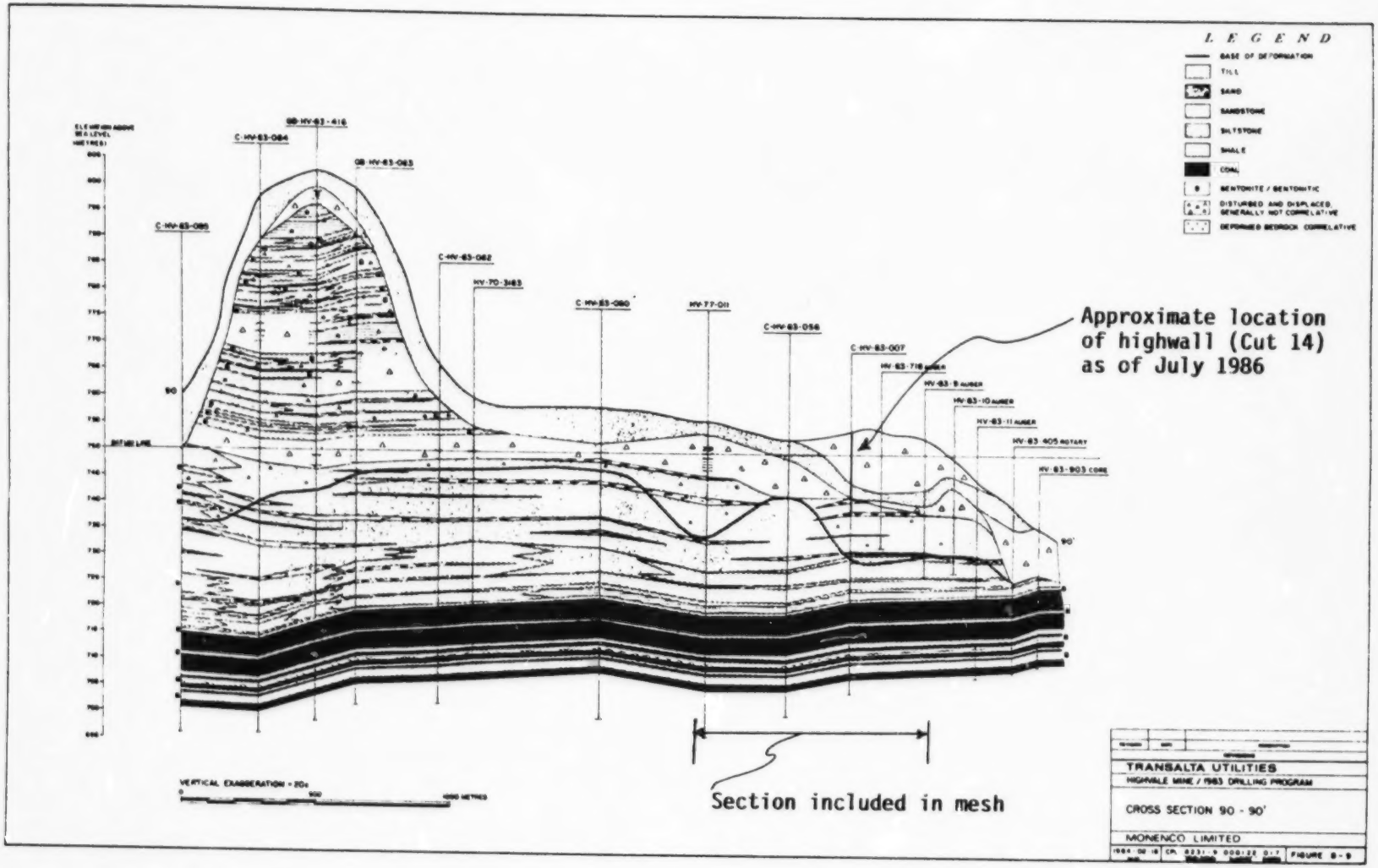

FIG. 2. Geologic cross-section of Highvale Mine at Pit 03

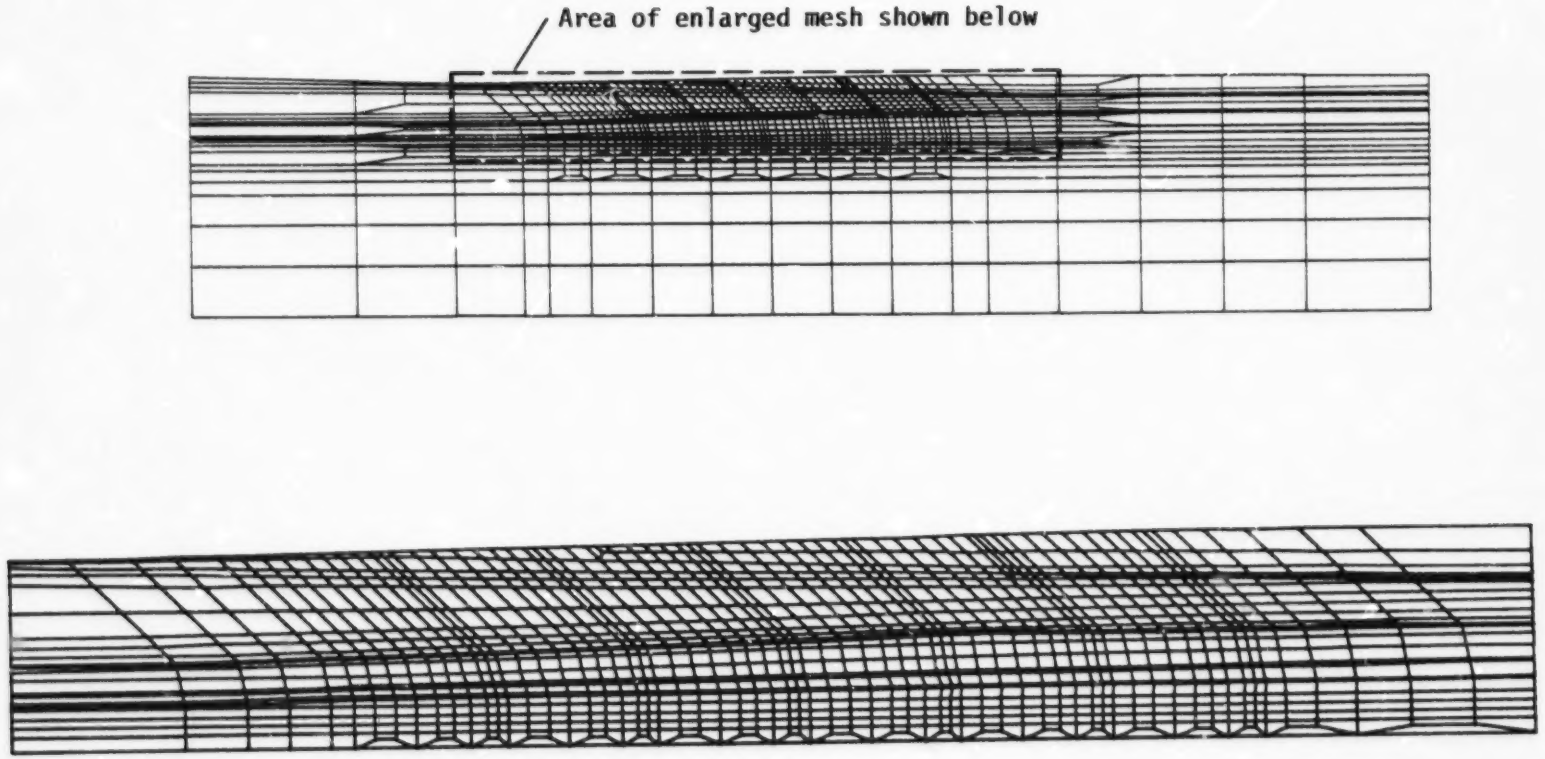

FIG. 3. Finite element mesh of REM model

TABLE 1. Highwall Position from June 1987 to May 1988

Cut No.	Crest of Highwall		Toe of Highwall	
	Elev. (m)	Northing* (m)	Elev. (m)	Northing (m)
17	742	1228	721	1247
18	741.5	1182	720	1202
19	743	1131	719	1155
20	745	1090	719	1116
21	∿745	∿1040	∿ 719	∿ 1076
22	∿745	∿ 990	∿ 719	∿ 1030

* Eastings are irrelevant since highwall was oriented east-west for each cut.

Source: C.A. Small, 6 October 1988.

o Excavation sequences. Excavation of the coal layers was simulated as occurring instantaneously with the bank and chop cuts. This is considered to be a worst-case situation. The Pit 03 REM model was developed to study five consecutive cuts/excavations over a period of about one year. In the model, all excavation activity that had occurred prior to the five excavation cycles was simulated by instantaneous excavation in a single stage. Creation of a spoil pile on the excavation ground was simulated by adding vertical loading on the surface of the newly mined pit floor. Table 2 shows the excavation stages employed in the current simulation.

TABLE 2. Excavation Stages in REM Model

Stage No.	Activities	Starting Day	Ending Day	Duration (days)
1	Consolidation	--	--	0
2	Cut 16	--	--	90
3	Cut 17	26 Jun 87	22 Aug 87	86
4	Cut 18	23 Aug 87	08 Nov 87	76
5	Cut 19	09 Nov 87	08 Mar 88	90
6	Cut 20	09 Mar 88	13 May 88	64

- Duration of simulation. The period of simulation extended from the first day of Cut 16 to the last day of Cut 20. Time periods between consecutive cuts are summarized in Table 2.

- External loading. The Highvale Mine dragline weighs about 2.8 million kg, which has a considerable effect on slope stability. The weight was converted to a load of 0.11 MPa (16.2 psi) acting on the bank cut with a length of 20 meters and a setback of 5 meters from the crest.

- In situ stress state. In the present study, a hydrostatic (lithostatic) in situ stress state in which lateral stress equals vertical stress was assigned to the model. The initial stress was calculated as a function of depth below the ground surface.

- Material properties. The REM material property set comprises 21 parameters that together simulate most of the critical behaviors of geologic materials: elasticity, viscoelasticity, viscoplasticity, compressibility, strength deterioration, failure, and post-failure. The material properties of the identified geologic strata were evaluated based on laboratory rock testing and Propertymeter field measurement results.

During model calibration, the preliminary material property sets were refined against field-measured deformation and the improved sets were later used in evaluation of designs with different slopes. The calibration work began by applying the initial material property sets shown in Table 3, which were used in the earlier project [2,3] under DSS Contract No. 23440-6-9021/01-SQ. The calibrated material property sets used later for design evaluation in the current project are given in Table 4.

- Water-table level. Information on ground-water level and the phenomenon of water-level drawdown near a freshly excavated slope was obtained from previous piezometric studies [5,6]. These studies established the water-table level as a function of month and season. Accounting for precipitation during the rainy months, a worst-case assumption thus was invoked and the highest water level incorporated into the model. The effect of ground water was considered by making adjustments to the material properties of the strata below the ground-water level. It was ascertained that the sandstone and bentonitic mudstone would be most affected by ground water. Each of the two materials was assigned two sets of material properties, one for partial and the other for total saturation. The former property set was defined based on the laboratory testing results and the latter was derived from SGI's data bank.

  Initially in unexcavated ground, the full-saturation properties were used for the sandstone and mudstone, the shaley siltstone and coal being assumed to be less vulnerable to ground water. The effect of water-level drawdown was simulated by changing the property set for affected elements of sandstone and mudstone to that corresponding to a partially saturated condition. This change was implemented according to the drawdown contour data obtained in the piezometric measurement program. It was also implemented simultaneously with the excavation of a fresh slope, neglecting the transient phenomenon for steady-state simulation.

TABLE 3. Preliminary Material Property Sets of REM Model

REM MATERIAL PROPERTY PARAMETERS			TILL	WEAK SANDST.	NORM SANDST.*	MUDST.*
DESCRIPTION	SYMBOL	UNIT	(Set 1)	(Set 2)	(Set 3)	(Set 4)
Shear modulus	G_1	psi	500	1000	11000	500
Retarded shear modulus ($\tau_o < K_o$)	G_2	psi	1000	1000	20000	2000
Retarded shear modulus ($\tau_o > K_o$)	G_3	psi	1000	1000	20000	2200
Elastoviscosity ($\tau_o < K_o$)	V_2	psi da	2000	2000	10000	2000
Elastoviscosity ($\tau_o > K_o$)	V_3	psi da	2000	2000	10000	4000
Plastoviscosity	V_4	psi da	4000	4000	60000	3800
Ultimate bulk modulus	K_1	psi	5000	8000	18000	5000
Retarded bulk modulus	K_2	psi	10000	10000	25000	8500
Hydrostatic elastoviscosity	D_2	psi da	30000	30000	50000	17000
Unconfined strength	K_o^A	psi	40	50	400	60
Ultimate octah. shear strength	K_o^B	psi	400	500	2400	300
Minimum octah. shear strength	K_o^{min}	psi	15	15	300	10
Yield surface coefficient	α	psi	0.005	0.007	0.01	0.005
Critical strain of failure	γ_o^c	--	0.03	0.03	0.01	0.04
Deterioration coeff. of shear	C	--	5	5	9	4
Unconfined bulk modulus	K_1^A	psi	400	600	1200	400
Minimum bulk modulus	K_1^{min}	psi	200	400	1000	300
Density gradient	ρ_y	psi/ft	-0.883	-0.978	-1.14	-0.80
Power coeff. of plastoviscosity	n	--	2.6	2.6	2.6	2.6

* Fully saturated

continues...

TABLE 3. Preliminary Material Property Sets of REM Model (continued)

REM MATERIAL PROPERTY PARAMETERS			COAL	SHALEY SILTST.	NORM SANDST.*	MUDST.*
DESCRIPTION	SYMBOL	UNIT	(Set 5)	(Set 6)	(Set 7)	(Set 8)
Shear modulus	G_1	psi	1000	1000	12000	600
Retarded shear modulus ($\tau_o < K_o$)	G_2	psi	2500	3000	20000	3500
Retarded shear modulus ($\tau_o > K_o$)	G_3	psi	2500	3000	20000	3000
Elastoviscosity ($\tau_o < K_o$)	V_2	psi da	2000	3500	10000	3000
Elastoviscosity ($\tau_o > K_o$)	V_3	psi da	2000	3500	10000	4000
Plastoviscosity	V_4	psi da	8000	8000	70000	4000
Ultimate bulk modulus	K_1	psi	7500	10000	20000	6000
Retarded bulk modulus	K_2	psi	8000	10000	30000	10000
Hydrostatic elastoviscosity	D_2	psi da	22000	30000	50000	17000
Unconfined strength	K_o^A	psi	200	200	500	60
Ultimate octah. shear strength	K_o^B	psi	500	500	2500	500
Minimum octah. shear strength	K_o^{min}	psi	100	100	500	10
Yield surface coefficient	α	psi	0.006	0.007	0.01	0.07
Critical strain of failure	γ_o^c	--	0.02	0.02	0.008	0.03
Deterioration coeff. of shear	C	--	6	7	10	4
Unconfined bulk modulus	K_1^A	psi	650	800	1500	400
Minimum bulk modulus	K_1^{min}	psi	400	600	1000	300
Density gradient	ρ_y	psi/ft	-0.606	-0.888	-1.138	-0.75
Power coeff. of plastoviscosity	n	--	2.6	2.6	2.6	2.6

* Partially saturated

TABLE 4. Calibrated Material Property Sets of REM Model

REM MATERIAL PROPERTY PARAMETERS			TILL	WEAK SANDST.	NORM SANDST.*	MUDST.*
DESCRIPTION	SYMBOL	UNIT	(Set 1)	(Set 2)	(Set 3)	(Set 4)
Shear modulus	G_1	psi	1000	2000	11000	500
Retarded shear modulus ($\tau_o < K_o$)	G_2	psi	2000	2000	20000	2000
Retarded shear modulus ($\tau_o > K_o$)	G_3	psi	2000	2000	20000	2200
Elastoviscosity ($\tau_o < K_o$)	V_2	psi da	4000	4000	10000	2000
Elastoviscosity ($\tau_o > K_o$)	V_3	psi da	4000	4000	10000	4000
Plastoviscosity	V_4	psi da	8000	8000	60000	3800
Ultimate bulk modulus	K_1	psi	10000	16000	18000	5000
Retarded bulk modulus	K_2	psi	20000	20000	25000	8500
Hydrostatic elastoviscosity	D_2	psi da	60000	60000	50000	17000
Unconfined strength	K_o^A	psi	40	50	400	50
Ultimate octah. shear strength	K_o^B	psi	400	500	2400	300
Minimum octah. shear strength	K_o^{min}	psi	15	15	300	10
Yield surface coefficient	α	psi	0.005	0.007	0.01	0.005
Critical strain of failure	γ_o^c	--	0.03	0.03	0.01	0.04
Deterioration coeff. of shear	C	--	5	5	9	4
Unconfined bulk modulus	K_1^A	psi	800	1200	1200	400
Minimum bulk modulus	K_1^{min}	psi	400	800	1000	300
Density gradient	ρ_y	psi/ft	-0.883	-0.97	-1.14	-0.80
Power coeff. of plastoviscosity	n	--	2.6	2.6	2.6	2.6

* Fully saturated

continues...

TABLE 4. Calibrated Material Property Sets of REM Model (continued)

REM MATERIAL PROPERTY PARAMETERS			COAL	SHALEY SILTST.	NORM SANDST.*	MUDST.*
DESCRIPTION	SYMBOL	UNIT	(Set 5)	(Set 6)	(Set 7)	(Set 8)
Shear modulus	G_1	psi	3000	3000	12000	600
Retarded shear modulus ($\tau_o < K_o$)	G_2	psi	7500	9000	20000	3500
Retarded shear modulus ($\tau_o > K_o$)	G_3	psi	7500	9000	20000	3000
Elastoviscosity ($\tau_o < K_o$)	V_2	psi da	6000	10500	10000	3000
Elastoviscosity ($\tau_o > K_o$)	V_3	psi da	6000	10500	10000	4000
Plastoviscosity	V_4	psi da	24000	24000	70000	4000
Ultimate bulk modulus	K_1	psi	22500	30000	20000	6000
Retarded bulk modulus	K_2	psi	24000	30000	30000	10000
Hydrostatic elastoviscosity	D_2	psi da	66000	90000	50000	17000
Unconfined strength	K_o^A	psi	200	200	500	60
Ultimate octah. shear strength	K_o^B	psi	500	500	2500	500
Minimum octah. shear strength	K_o^{min}	psi	100	100	500	10
Yield surface coefficient	α	psi	0.006	0.007	0.01	0.07
Critical strain of failure	γ_o^c	--	0.02	0.02	0.008	0.03
Deterioration coeff. of shear	C	--	6	7	10	4
Unconfined bulk modulus	K_1^A	psi	2000	2400	1500	400
Minimum bulk modulus	K_1^{min}	psi	1200	1800	1000	300
Density gradient	ρ_y	psi/ft	-0.606	-0.888	-1.138	-0.75
Power coeff. of plastoviscosity	n	--	2.6	2.6	2.6	2.6

* Partially saturated

Model Calibration

In the present study, finite elements were used to discretize the continuum in the space domain, the three-dimensional problem was reduced to two dimensions under the plane strain idealization, and the finite difference technique was applied to approximate exact solutions in the time domain. The material properties initially assigned were based on the 1987 rock testing results [1]. In view of the limited nature of the rock testing program, these properties were adequate only for preliminary representation of the complex geological strata of Highvale Mine. The material properties were then refined through back analysis in an effort to match the computer results with the field-measured ground behavior over a period of five consecutive cuts.

- Deformation data. The field deformation data used in calibration were provided by the University of Alberta [4]. The deformation monitoring program was accomplished using six primary vertical inclinometers (S1 through S6) installed on 50-meter centers with survey control from two reference points. Figs. 4 and 5 show the layout and north-south profile of the site as it appeared from June through September 1987. The topographic changes resulting from a new excavation cycle in September 1987 are illustrated in Figs. 6 and 7. Table 5 summarizes movement at the elevation of 730 meters for the six inclinometers. The listed movements were approximated from estimations made at the base of the inclinometers, with addition of known movements in shear zones above the coal seams.

- Calibration. The six inclinometers were deployed at three different positions on the north-south profile, as shown in Fig. 8. The paired instruments S1 and S2, S3 and S4, and S5 and S6 had the same northern coordinates, respectively. Pairs of inclinometers having the same northern coordinates were considered as a unit in calibrating against the computer-projected results because of the two-dimensional configuration of the REM model. Figs. 9 through 11 show the computer-projected

TABLE 5. Movement at Elevation 530 meters
(Estimated from Inclinometer Readings)

SUMMARY OF MOVEMENTS AT ELEVATION 730 metres						
	DAY 10		DAY 36		DAY 44	
REFERENCE POINT	DIST. FROM H/W CREST	NORTH MOVEMENT	DIST. FROM H/W CREST	NORTH MOVEMENT	DIST. FROM H/W CREST	NORTH MOVEMENT
S1	97	70	97	79	97	81
S2	95	70	95	73	95	82
S3	148	35	148	39	148	45
S4	143	35	143	40	143	43
S5	200	15	200	14	200	17
S6	192	15	192	16	192	20
BM1	300	1	300	1	300	1
BM2	300	1	300	1	300	1

	DAY 57		DAY 71		DAY 92	
REFERENCE POINT	DIST. FROM H/W CREST	NORTH MOVEMENT	DIST. FROM H/W CREST	NORTH MOVEMENT	DIST. FROM H/W CREST	NORTH MOVEMENT
S1	97	92	97	93	51	97
S2	95	91	95	87	49	98
S3	148	48	148	44	102	47
S4	143	45	143	46	97	53
S5	200	19	200	20	154	22
S6	192	23	192	24	146	31
BM1	300	1	300	1	250	2
BM2	300	2	300	2	250	10

	DAY 118		DAY 150		DAY 155	
REFERENCE POINT	DIST. FROM H/W CREST	NORTH MOVEMENT	DIST. FROM H/W CREST	NORTH MOVEMENT	DIST. FROM H/W CREST	NORTH MOVEMENT
S1	51	148	51	178	.	.
S2	49	188	49	223	.	.
S3	102	64	102	81	102	79
S4	97	68	97	98	97	92
S5	154	29	154	40	154	38
S6	146	39	146	52	146	49
BM1	250	2	250	2	250	2
BM2	250	10	250	10	250	10

continues...

TABLE 5. Movement at Elevation 530 meters (Estimated from Inclinometer Readings) (continued)

REFERENCE POINT	DAY 173		DAY 211		DAY 238	
	DIST. FROM H/W CREST	NORTH MOVEMENT	DIST. FROM H/W CREST	NORTH MOVEMENT	DIST. FROM H/W CREST	NORTH MOVEMENT
S1	0	275	0	331	0	360
S2	-2	314	-2	406	-2	398
S3	51	106	51	109	51	120
S4	46	178	46	189	46	201
S5	103	21	103	55	103	57
S6	95	38	95	77	95	85
BM1	200	6	200	7	200	8
BM2	200	21	200	22	200	23

REFERENCE POINT	DAY 268		DAY 295		DAY 309	
	DIST. FROM H/W CREST	NORTH MOVEMENT	DIST. FROM H/W CREST	NORTH MOVEMENT	DIST. FROM H/W CREST	NORTH MOVEMENT
S1	.	.	.	.	.	.
S2	.	.	.	.	.	.
S3	10	137	10	218	10	247
S4	5	308	5	353	5	409
S5	62	104	62	111	62	137
S6	54	128	54	152	54	178
BM1	150	33	150	35	150	46
BM2	150	54	150	56	150	71

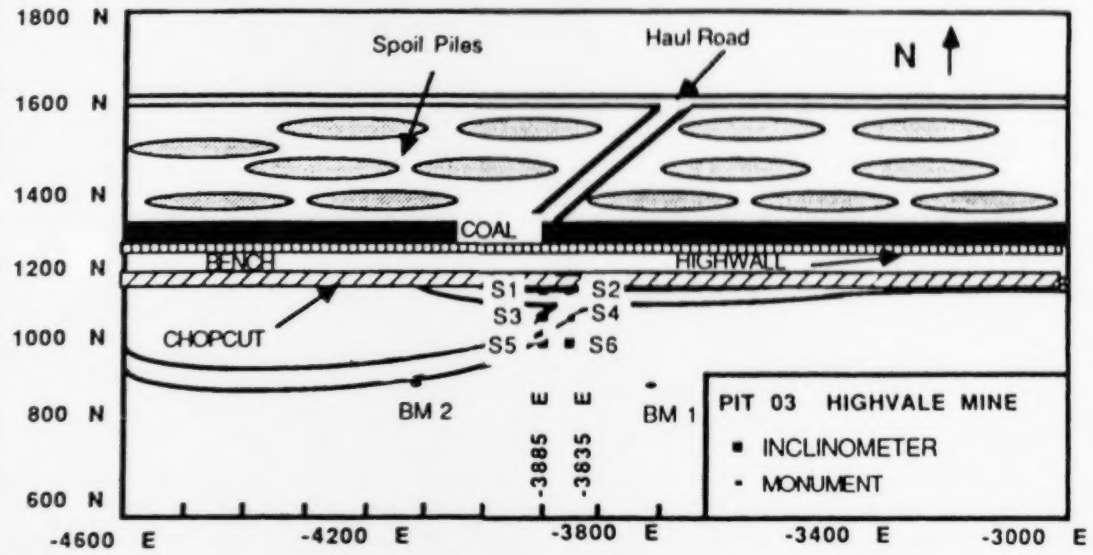

Figure 4 . Plan view of study site from June to September 1987

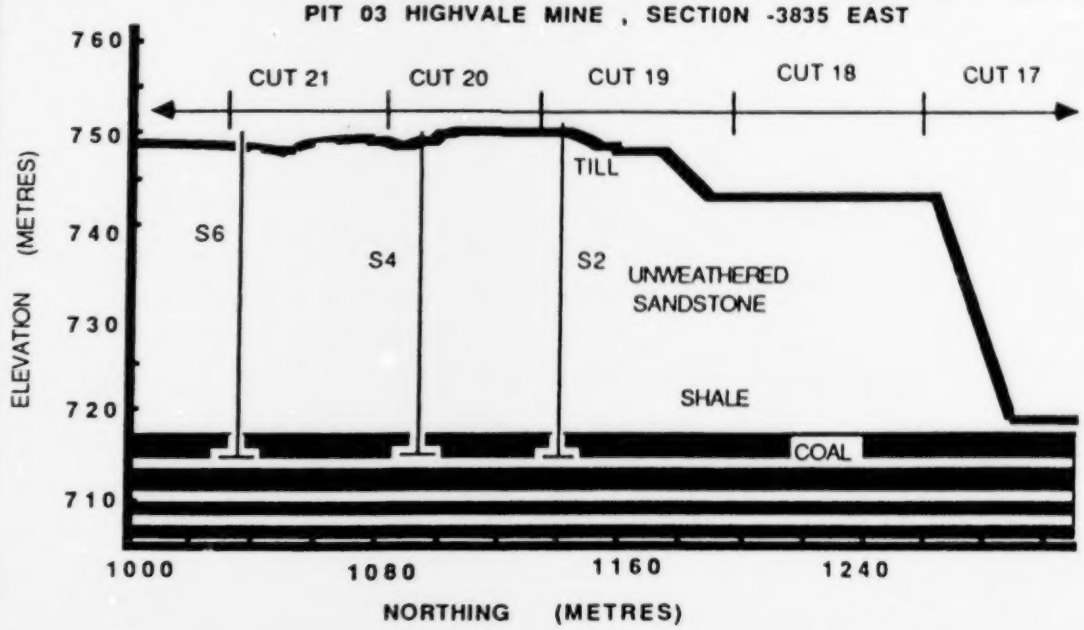

Figure 5 . Cross section through -3835 East, June to September 1987

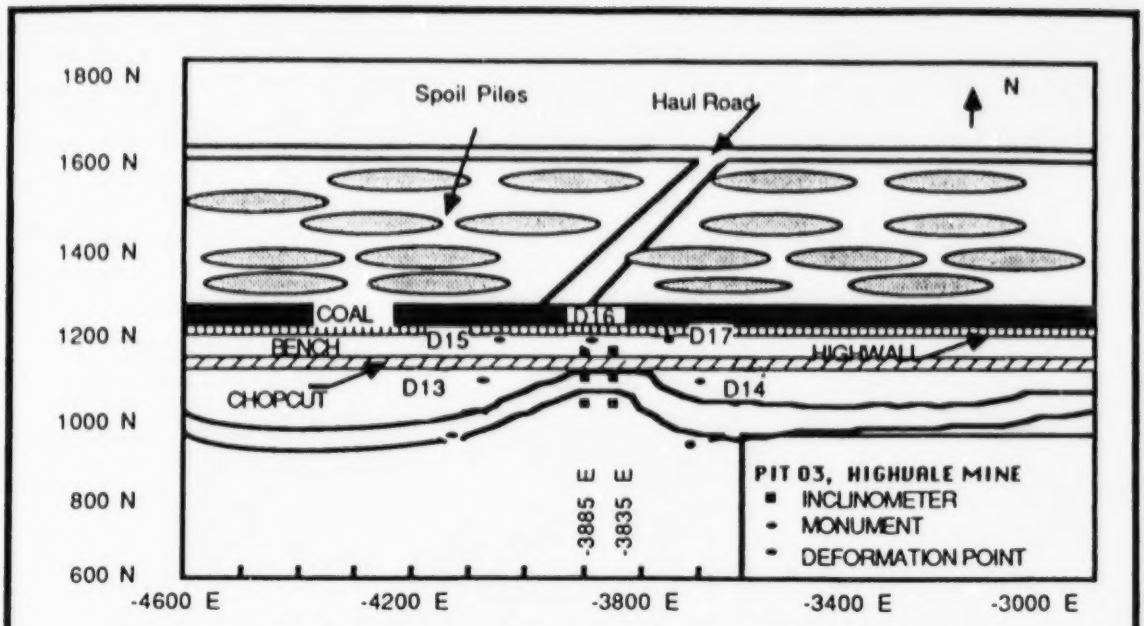

Figure 6 . Plan view of study site from September to December 1987.

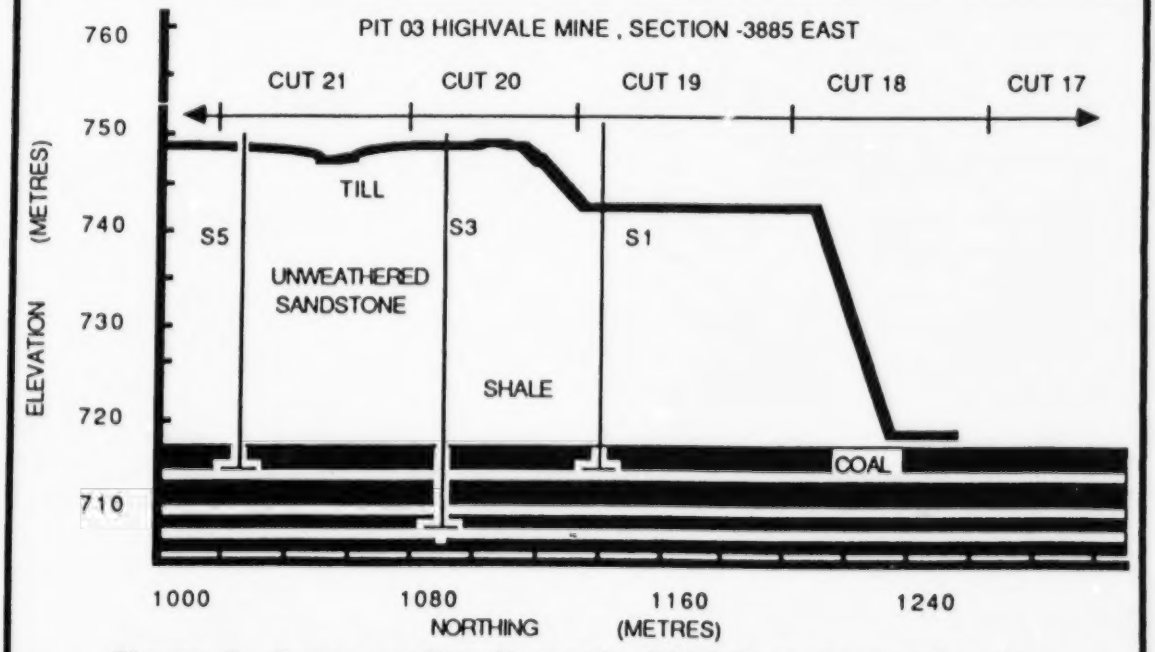

Figure 7 . Cross section through -3885 East, September to December 1987.

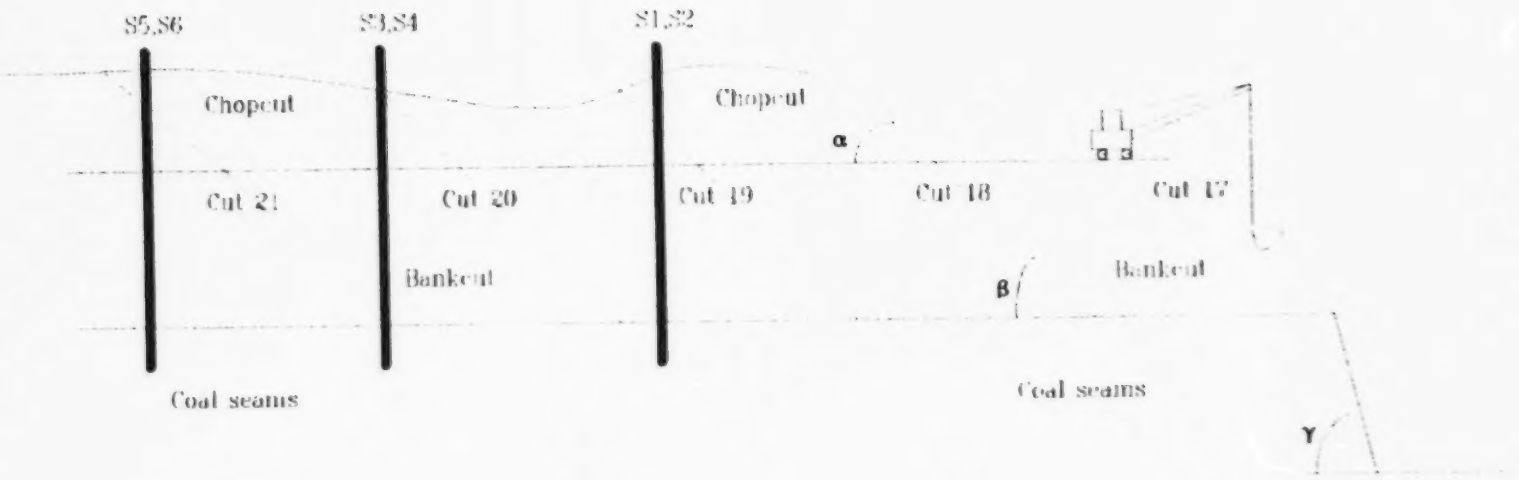

FIG. 8. Positions of inclinometers in typical north-south profile

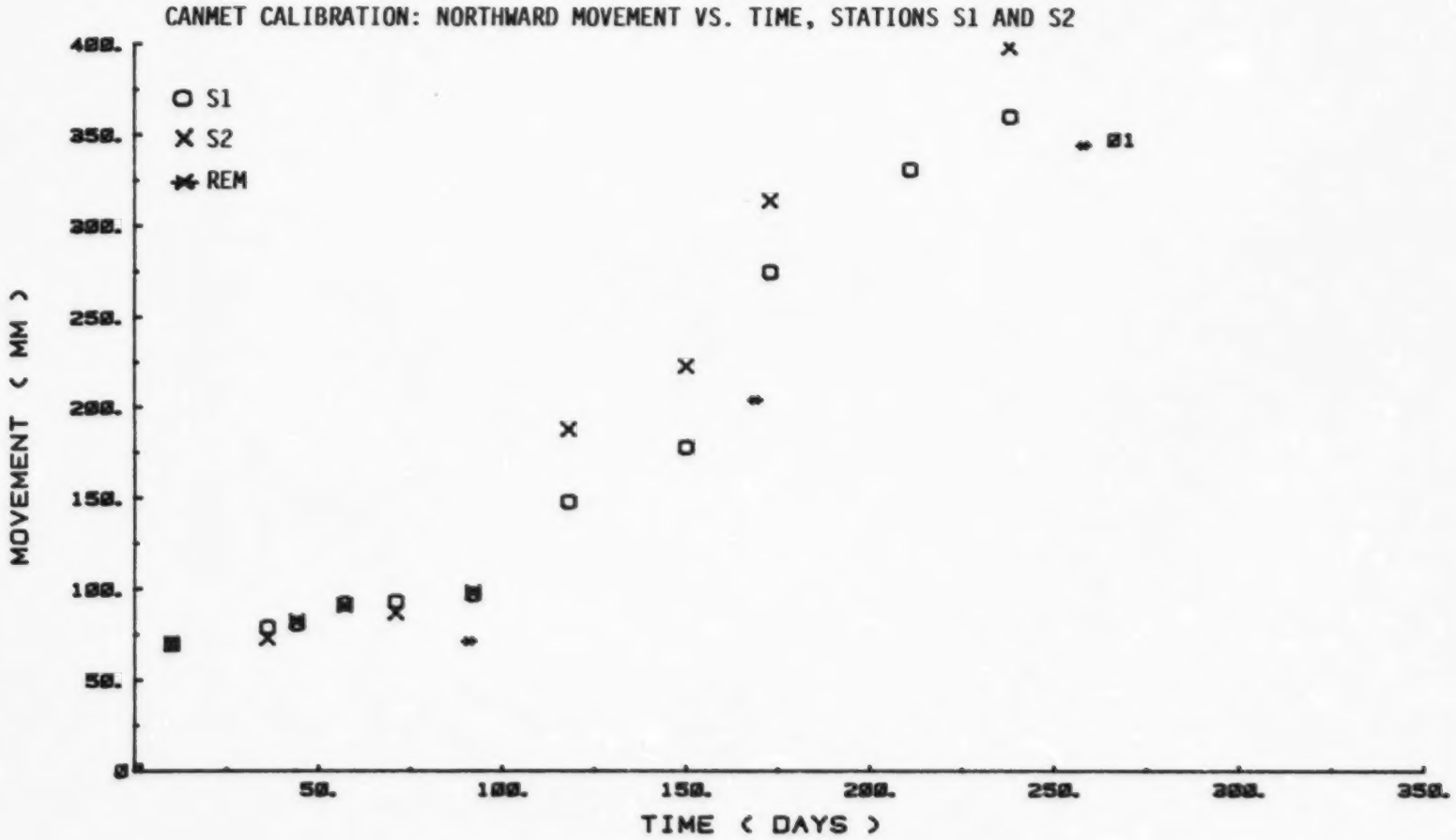

FIG. 9. Northward movement of stations S1 and S2 at Elevation 730 meters, with REM projection

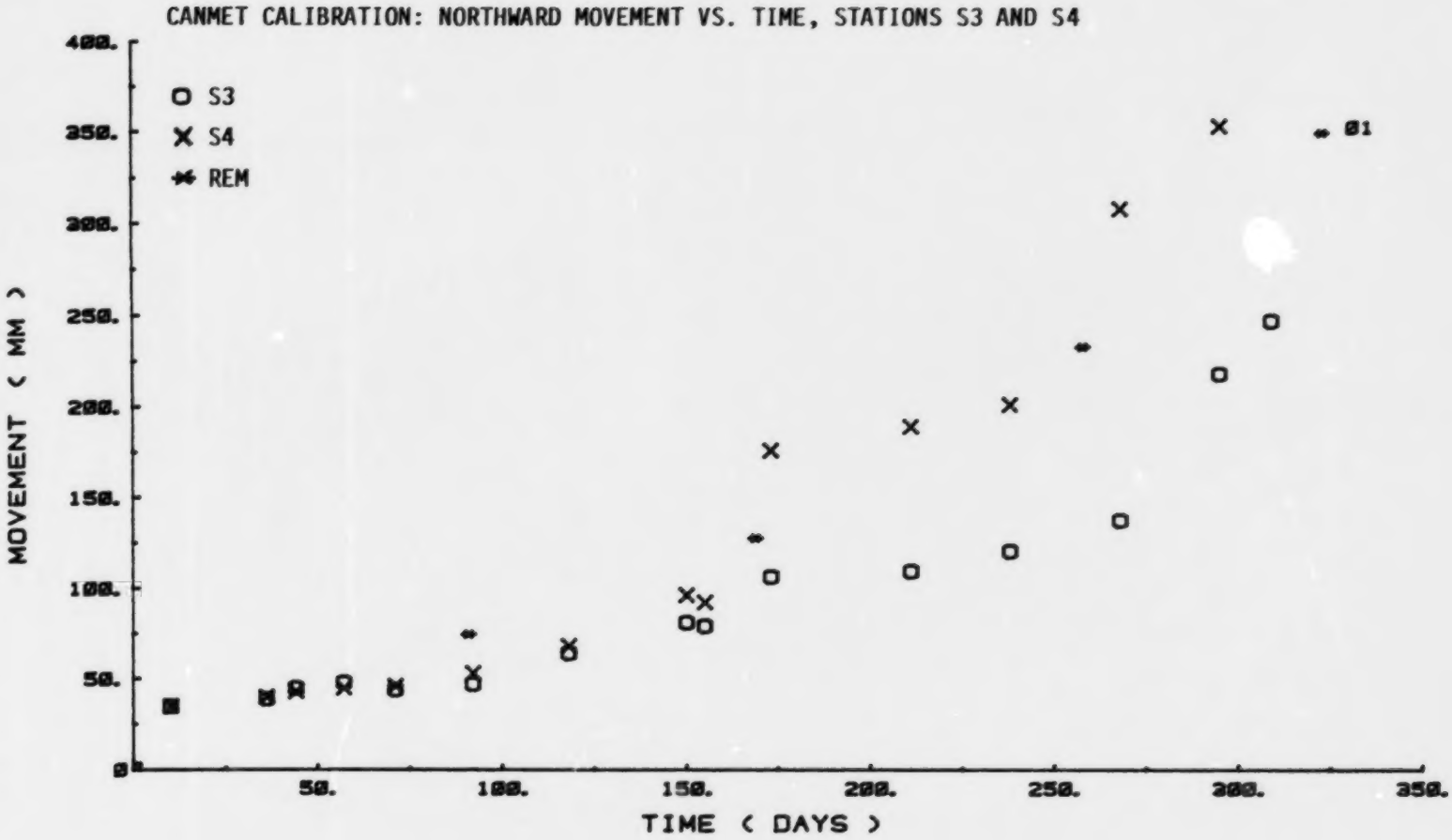

FIG. 10. Northward movement of stations S3 and S4 at Elevation 730 meters, with REM projection

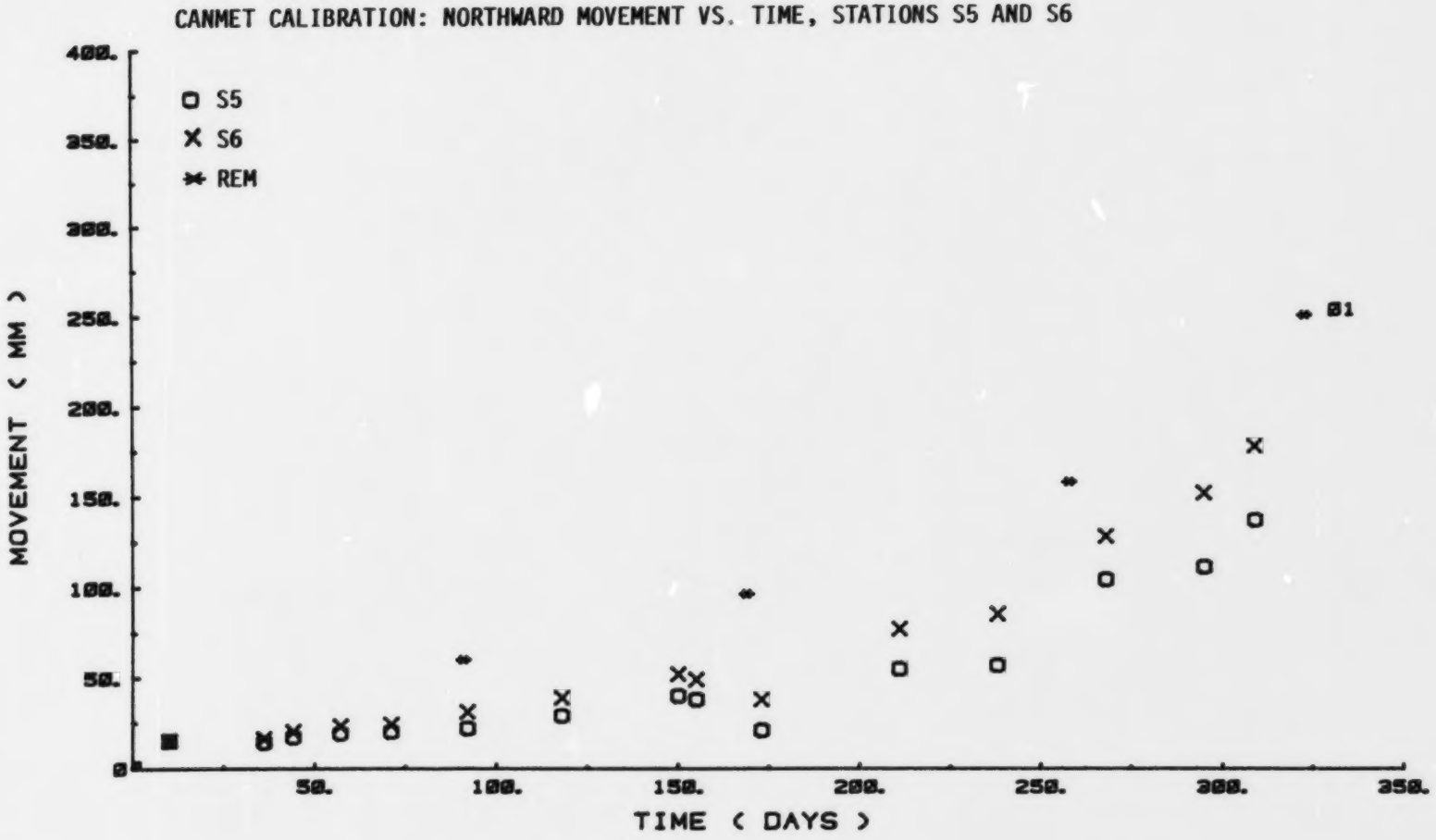

FIG. 11. Northward movement of stations S5 and S6 at Elevation 730 meters, with REM projection

deformations as well as the field-measured movements at the elevation of 730 meters for the three station pairs. The REM projections matched the field data very well except for the slight overestimation of the stations farthest from the highwall (S5 and S6). The calibration process illustrated the ability of REM to simulate continuous open-pit mining. It should be noted that some of the field data themselves exhibit discrepancy (e.g., between the data from S3 and S4) due to the highly varied glaciotectonic geology of Highvale Mine, which indicates that refinement of material properties will be required before the model can be applied effectively for slope design evaluation in other areas.

5.0 EVALUATION OF PIT DESIGNS

Design Variants

The prior study under Contract No. 23440-6-9021/01-SQ focused on application of the computer model to a set of design variants, as follows:

- Material properties
- Initial stress state
- Excavation sequence
- Excavation timing
- Pit slope geometry.

Material properties and initial stress state, i.e., the inputs representing the natural characteristics of the mine ground, were established through calibration. In all cases, excavation sequence was assigned the most critical condition -- simultaneous excavation of the overburden and coal -- to ensure conservative analysis. Time between two consecutive cuts was kept at three months in accordance with recent mining activities. Therefore, pit slope geometry was the only parameter varied for evaluation of different designs.

Three sets of slope angles analyzed in the previous project were evaluated again in the present study. Table 6 summarizes the three pit design variants which are defined in Fig. 12 as α, β, γ.

TABLE 6. Pit Design Variations for REM Simulation

Run No.	Chop Cut Angle α	Bank Cut Angle β	Excavation Angle γ
1	45°	57°	80°
2	50°	65°	
3	55°	72°	

Simulation Results

The numerical analysis yielded strain and deformation results, which are important indexes for stability analysis. This information is depicted graphically in Appendix B in a form that highlights areas of engineering interest. For each computer run, the following plots are presented:

- Contour of octahedral shear strain
- Principal strain distribution
- Deformed mesh of final slope
- Displacement of critical nodes over time.

The REM model simulated five successive cuts, the last being of greatest interest. The four plots obtained for each of three runs, as summarized in Appendix B, present the results for the final cut in terms of its slope and behavior. For each run, the first three plots focus on an area just behind the exposed face of the slope, while the fourth presents the displacement of critical points on the open face of the coal above the pit floor.

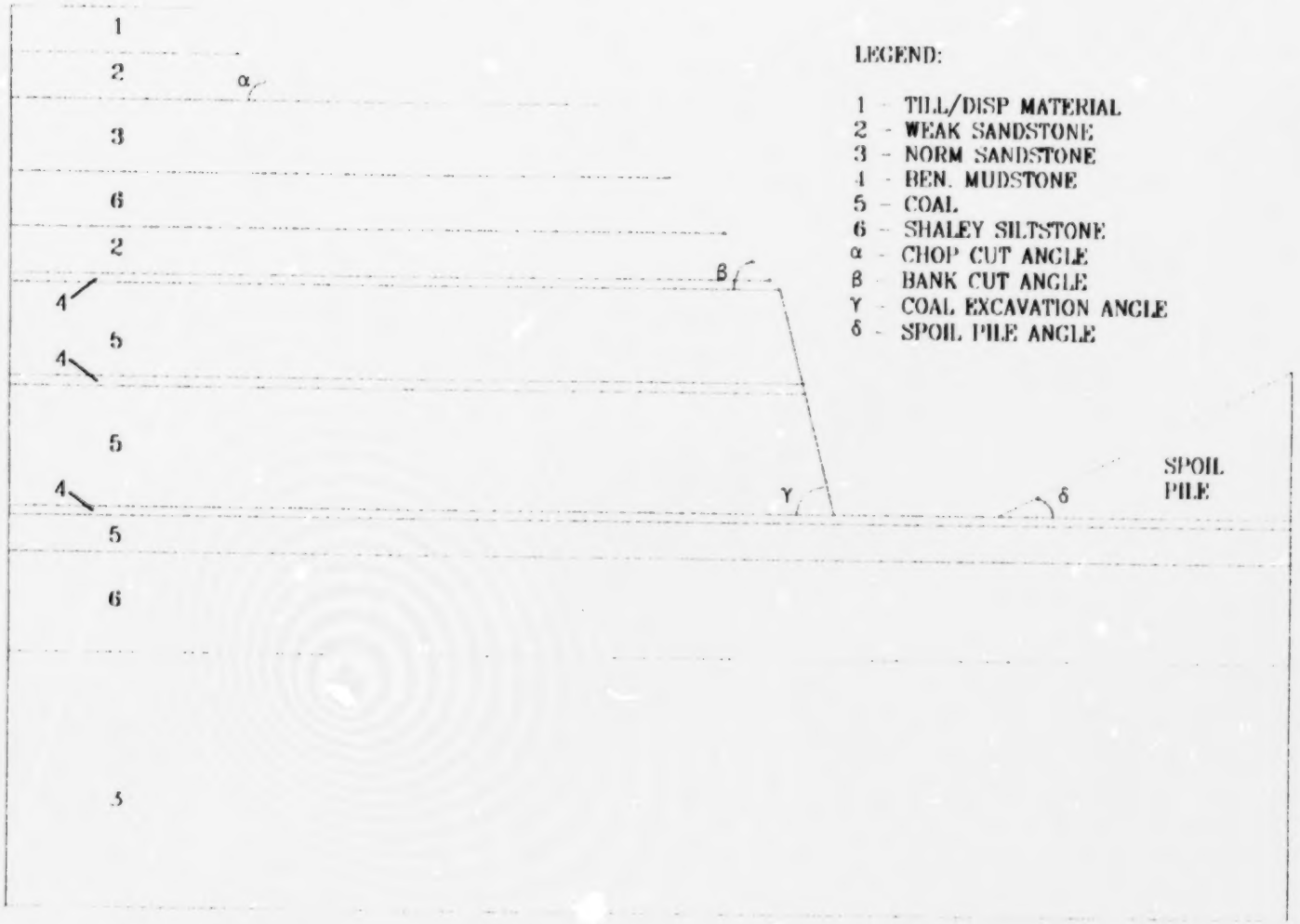

FIG. 12. Material types and slope geometry parameters incorporated in REM model

The run designations given in Table 6 are referenced to the figures in Appendix B. For comprehensive analysis incorporating comparisons between different simulations, three critical parameters were extracted from these plots:

- Maximum displacement, δ_{max}
- Maximum octahedral shear strain, γ_{max}
- Maximum principal strain, ε_{max}.

The values of these parameters from the present and previous studies are given in Table 7.

TABLE 7. Maximum Values of Critical Parameters Projected in REM Simulations

Run No.	Index	Previous Study	Present Study
1	δ_{max}	0.48 m	0.188 m
$\alpha = 45^{o}$	γ_{max}	12%	7%
$\beta = 57^{o}$	ε_{max}	20%	7.5%
2	δ_{max}	0.48 m	0.208 m
$\alpha = 50^{o}$	γ_{max}	14%	7%
$\beta = 65^{o}$	ε_{max}	19%	7.6%
3	δ_{max}	0.48 m	0.219 m
$\alpha = 55^{o}$	γ_{max}	14%	7%
$\beta = 72^{o}$	ε_{max}	19%	7.7%

Discussion

Since great effort had been expended on the parametric study under DSS Contract No. 23440-6-9021/01-SQ, the focus of the present work was to reassess the recommendations made in that project by applying the calibrated

REM model in computer simulations. The improved model employs much stronger material properties and, therefore, lower strain and deformation values are predicted by the calibrated model despite the additional dragline loading now implemented.

Table 7 shows clearly that 1) the maximum value of principal strain projected in the improved model is about one-third of the value obtained by the earlier model, 2) the maximum value of octahedral shear strain in the improved model is half that in the prior model, and 3) the maximum displacement due to the last cut is now reduced to 20 cm compared to 50 cm in the prior model. The low values of all three indexes for evaluating slope stability confirm the safety of those designs which were determined to be safe under the preceding contract.

The present study shows only slight sensitivity to changes in the slope angles, which also agrees with the conclusion of the previous slope angle study.

As was concluded in the earlier study, material properties are shown to be a more dominant factor than the slope angles, and thus the REM model for Highvale Mine design simulation is highly site-specific due to the localized geologic effects caused by glaciotectonic forces. Fine-tuning of the model will be necessary whenever a change of ground property is detected. Seasonal effects on ground conditions should be incorporated, especially considering that increased pore-water pressure results in decreased material strength and greater probability of slope failure. In addition, heavily jointed areas warrant careful slope redesign with smaller angles to prevent aggravation of instabilities.

6.0 CONCLUSIONS

The REM constitutive model has been demonstrated to be capable of predicting the behavior of mine ground in response to mining activities. A site-specific finite element model of the Highvale Mine ground was constructed and calibrated by integrating previous laboratory testing and field measurement programs. Three different pit designs were evaluated by applying the calibrated model to finite element simulation. The computer-projected results showed less deformation than did the preliminary model developed under DSS Contract No. 23440-6-9021/01-SQ. Therefore, the prior recommendations regarding design variants from the safety point of view are confirmed.

The following conclusions, drawn from the present study as well as the previous report, summarize the stability studies performed by SGI for Highvale Mine Pit 03:

1. Stability of the pit slope depends greatly on the ground material properties. The effect of environmental conditions, joints, weak zones, and other factors should be considered closely with respect to material properties for their influence on slope stability.

2. Slope angles appeared not to be a sensitive design parameter, although ground deformation did increase for steeper slope angles.

3. Excavation timing was shown to have a significant effect on slope stability. Greater strains and deformations accumulated during the simulations that had greater intervals between successive excavations.

4. Simultaneous removal of coal and overburden was a worst-case scenario and caused greater strain damage at the toe of the slope.

5. Excess lateral stresses resulted in higher strain and deformation, and consequently in a greater risk of slope failure.

6. The three pit designs evaluated in the current study appear to be globally safe under the assigned conditions. The same computer model can be utilized in pit design optimization for other sites with appropriate adjustments to the geology, material properties, and stress input.

Specific Design Considerations

According to the samples extracted in holes HV-86-901 and 902 [1], it is likely that an area of stronger sandstone will be encountered in Pit 03 as mining advances. If desired, pit slopes could be made steeper there to take advantage of the increased stability afforded by the stronger sandstone.

The other parameter requiring consideration for safe design is the cut height for a given slope. In the present study, the height of the bank cut was modeled as less than 20 meters. Any proposed increase in the highwall height of a bank cut should first be evaluated through simulation for the desired stability, using an adjusted model.

Given a dragline weight of 2.8 million kg, the potential for local failures caused by dragline operation merits detailed study. In the present computer model, the dragline was assigned a setback of 5 meters, following current mining practice. The dragline should be operated as smoothly as possible to minimize impact force and eccentric loadings, which will also reduce the likelihood of local failure. Inclining the bench slightly inward toward the next chop cut is suggested so that the lateral component of dragline weight will work in favor of highwall stability.

Areas with weak materials, joints, and discontinuities must be mined with shallower angles to optimize stability. Longer intervals between excavation, if foreseen, should be accommodated by reducing the slope angles. Likewise, retention of the coal for a few weeks after the chop cut and bank cut will improve slope stability.

7.0 RECOMMENDATIONS

Development of Site-Specific Design Criteria

The latest REM computer model developed in this study should be applied to formulate highly site-specific criteria for design and implementation of the excavation, through more systematic parametric analysis incorporating the following variables:

- o Geological variation
- o Critical material properties of bentonitic mudstone and shaley siltstone
- o Time sequence of excavation
- o Slope angles of α, β, and γ for chop cut, bank cut, and coal excavation, respectively.

Improvement of Field Measurements

The present program of benchmark and inclinometer measurements should be expanded to include monitoring of ground movement of selected pits where geomechanical conditions differ. Further, a new phase of field measurements should be instituted, using the now-computerized system of *in situ* stress-property measurement as described in the attachment, "SPDR Technology -- New Quantitative Methods in Geomechanics." The computerized SP-200 system replaces the earlier manual system SP-100, following significant improvements in both the quality and quantity of data collection as described in the attachment. In determining the material properties to be used as input to the REM model of the ground, the SP data obtained in the new measurement program should be supplemented by geophysical measurements.

Technology Transfer

The calibrated REM program should be transferred to the engineering group of TransAlta Utilities for immediate use and continued refinement of the model. TransAlta's engineers will be trained by SGI in the use of the REM program on a 386-type PC.

Extension of Model to Other Grounds

The site-specific REM program developed under the present effort, along with the proposed technology transfer, can be extended to other mines with significantly different geological and operational conditions. This may include both open-pit and underground mining of coal as well as other minerals.

8.0 REFERENCES

1. Serata Geomechanics, Inc., 1987, "Field/laboratory testing report," prepared for CANMET, March.

2. Serata Geomechanics, Inc., 1987, "Model development report," prepared for CANMET, April.

3. Serata Geomechanics, Inc., 1987, "Final report," prepared for CANMET, April.

4. Small, C.A. and Peterson, A.E., 1988, "Monitoring highwall deformations," Department of Civil Engineering, University of Alberta, Edmonton.

5. Monenco, Ltd., 1986, "Highvale Mine: 1985 geological and geotechnical data collection report," prepared for TransAlta Utilities, February.

6. Monenco, Ltd., 1987, "Highvale Mine: 1986 geological and geotechnical data collection report," prepared for TransAlta Utilities, January.

Appendix A

SPDR Technology

QUANTITATIVE ROCK MECHANICS IN COMPLEX GROUND: THE SPDR TECHNOLOGY

by

Shosei Serata, Ph.D.
and Shozo Sakuma*

INTRODUCTION

A quantitative means for reliable design, effective planning, and accurate cost estimating of rock mechanics work has not been available to civil engineers because of the complex nature of ground formations. For too long, engineers have depended solely on intuition and judgment based on experience in their practice. A new approach called the SPDR Technology® now enables engineers to quantify the design parameters related to underground structures.

The SPDR Technology expressly acknowledges that real ground behavior is far from ideally elastic; rather, it is dominated by the prefractured and time-dependent nature of the ground. Indeed, most ground is a hodgepodge of microfractures, local anomalies, and other nonelastic characteristics. Civil engineers generally do not have the opportunity to study the failure behavior of their projects -- except in highly unfortunate circumstances.

For this reason, it has been necessary to turn to mining ground in developing the new technology. The real world of underground mines and surface mining slopes has provided the experimental laboratory for close examination of actual ground conditions and behavior.

The outcome of more than 30 years of mine investigations is a technology that combines in situ measurement of stress state (S), material properties

---

* Shosei Serata, M.ASCE, is President of Serata Geomechanics, Inc., Richmond, California. Shozo Sakuma is Technical Director of JDC Corporation, Tokyo.

(P), and ground deformation (D) with a rheological finite element program (R) that is capable of comprehending the complex behavior of actual ground. The SPDR Technology has been validated *in situ* and applied over time at numerous mines, resulting in development of the Stress Control Method of mining [1,2]. As demonstrated in the mining industry, this approach is a powerful tool for the quantitative design and analysis of earth structures such as tunnels, underground spaces, slopes, dams, and foundations.

BACKGROUND

It is generally conceded that the finite element (FE) method has serious limitations when applied to rock mechanics problems in complex ground. This state of affairs was elaborated by Thomas R. Kuesel in his recent pair of *Civil Engineering* articles on tunneling [3]. Kuesel suggests that the difficulties in applying FE techniques can be attributed to the intrinsic complexities of rock media, which do not conform to conventional theories of soil mechanics and rock mechanics. His suggestion to civil engineers, expressed figuratively, was that it is futile to search for the key to the solution on the well lit side of the street when you know that the key is on the poorly lit side.

Conventional FE modeling of prefractured ground employs back analysis of deformation (D) data, attempting to match the D data with the model simulation results using assumed stress state (S) and assumed material properties (P). Unfortunately, practice has shown that dependence on such assumptions renders an FE model unrealistic and difficult to apply. In attempting to overcome this, numerous techniques have been tried for determining actual site-specific values of S and P *in situ*. However, such efforts have not previously succeeded in complex ground.

Responding to the clear need for direct *in situ* measurements, Serata Geomechanics, Inc. (SGI) has invented and built a set of S, P, and D measuring devices. SGI has also developed and refined a rheological FE

computer code REM® (R) for representation of earth material behaviors. The relationship among the four elements (S,P,D,R) is established by the SPDR Technology, which may be expressed in the following symbolic form:

$$S * P \xrightarrow{R} D$$

Here, the stress state (S) present in a geological formation interacts with the formation's material properties (P), producing ground deformation (D). The mechanism of this process is comprehended quantitatively by the REM computer model (R). The success of this approach over a wide range of applications is attributable to the rigorous quantitative basis established *in situ* for each of the four elements, as described below.

STRESS-PROPERTY MEASUREMENT SYSTEM

Field experience reveals that the stress state and material properties of a formation are closely related. *In situ* S is strongly affected by P; conversely, knowledge of P can be obtained from measurement of S. That is, by measuring the stress state we can evaluate the actual mass material properties of large, complex media which cannot be acquired otherwise.

In order to capture S and P together *in situ*, SGI introduced the stress-property measurement system SP-200. Figs. 1 and 2 illustrate the system and its components. The system employs a pair of interchangeable probes, the Stressmeter (S probe) and Propertymeter (P probe), which are applied in a single NX-size borehole.

The S probe consists of a loading cylinder in which are embedded eight LVDT sensors, deployed to measure the diametral deformation of the borehole at 45° angular intervals with accuracy on the order of 0.5 micron. The probe is activated hydraulically, similar to conventional pressuremeters commonly used in soil work. The P probe consists of a solid metal cylinder housing a set of eight loading pistons, which perform eight independent penetration

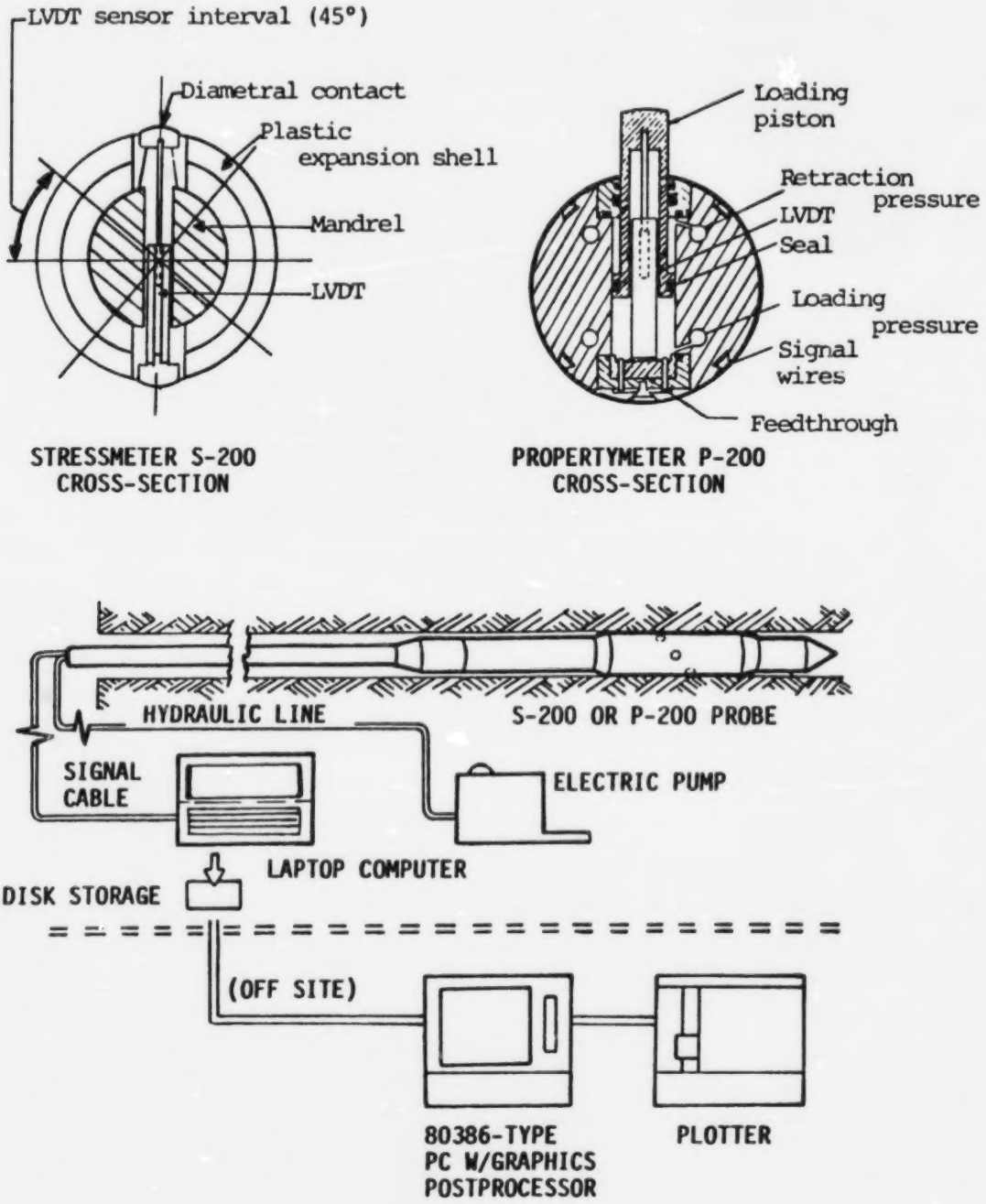

FIG. 1. Serata stress-property measurement system SP-200 showing cross-sections of interchangeable S-200 and P-200 probes

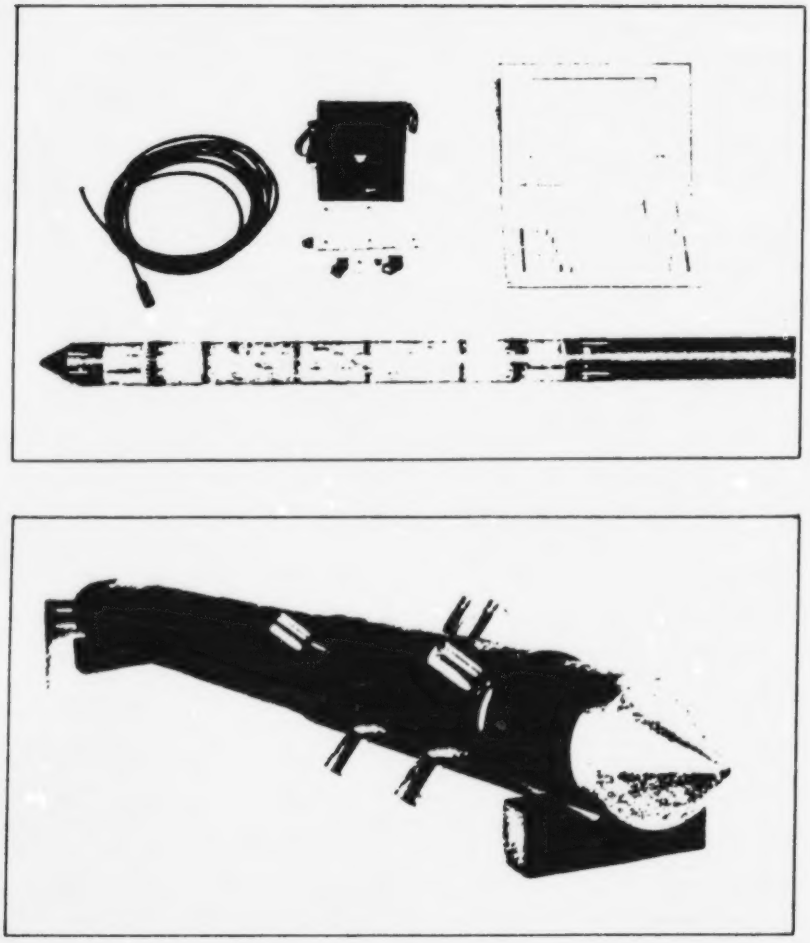

FIG. 2. Stressmeter S-200 with accessories (top) and Propertymeter P-200 (bottom)

tests against the face of the borehole. Each probe is equipped with gravity and magnetic field sensors for accurate spatial orientation in the borehole.

The S and P measurements are obtained automatically upon probe activation by the field technician, using a laptop computer as the operating console. Data are collected and processed instantaneously in the probes, then are transmitted by electrical cable to the computer for analysis and graphical display in real time on site. This enables the operator to evaluate the quality of measurement immediately while testing continues. With either probe, a set of measurements can be completed within a few minutes. The flexibility and speed of measurement permit the operator to deal effectively with any anomaly problems during the measurement process, not later at the office.

IN SITU MATERIAL PROPERTIES (P)

Determination of *in situ* material properties for FE modeling of earthwork requires an innovative approach. The S and P probes measure the basic material property coefficient values of failure strength, elastic coefficients, and creep properties realistically and economically in a given borehole. The material property values obtained by the two probes may differ from one another and also from laboratory test results of core specimens obtained from the same borehole. The differences disclose the critical information needed for FE computer modeling of the groundwork: that is, *in situ* material properties vary greatly according to the dimension of consideration in a highly site-specific manner.

For example, the dimensions of interaction for the S and P probes are those of the loading contact surfaces: 1.0 m for S and 0.01 m for P. The dimension for an underground tunnel is the size of the opening. This means that the P values obtained by the P probe represent point properties at the piston contact, while P obtained by the S probe represents mass properties

around the borehole boundary. These P values are yet different from the P of the rock masses surrounding the tunnel. As shown in Fig. 3, a relationship exists among the different material property values (failure strength is used as the example). The point properties are scattered widely, reflecting the fractured nature of the media. The mass properties, on the other hand, fall generally near the midpoint of the scatter of the point properties. Laboratory test values for core specimens typically approach the maximum because they usually represent intact rock. By utilizing the dimensional relation of P data obtained by the S and P probes, in situ mass properties of fractured ground can be estimated reliably. This realistic approach to the measurement of complex rock properties in situ is an essential element of the SPDR Technology.

STRESS MEASUREMENT IN COMPLEX GROUND (S)

Another essential for quantification of rock mechanics work is the ability to measure in situ stress states in complex ground, such as brittle-fractured rock and ductile-yielding media. The SP-200 system provides reliable, simple, and economical stress measurement. For application to brittle-fractured rock, use of the S probe alone is sufficient based on the "Multiple Fracture Method." For application to ductile-yielding media, both the S and P probes are required in accordance with the "SP Method."

In brittle-fractured rock, the S probe applies hydraulic loading up to 70 MPa to the borehole boundary through its plastic cylinder. Load/unload cycles are repeated, consolidating micro- and macro-fractures inherent in the rock around the borehole. Through the cyclic application of uniform loading, multiple fractures are induced in a mutually perpendicular orientation, as illustrated in Fig. 4. The first fracture plane (or a set of many subfractures conforming to the plane) is induced in the direction of the maximum stress (P_o); the second, in the direction of the minimum stress (Q_o). The two artificial fracture planes open at two different pressure points, p_1^E and p_2^E, representing the first and second planes,

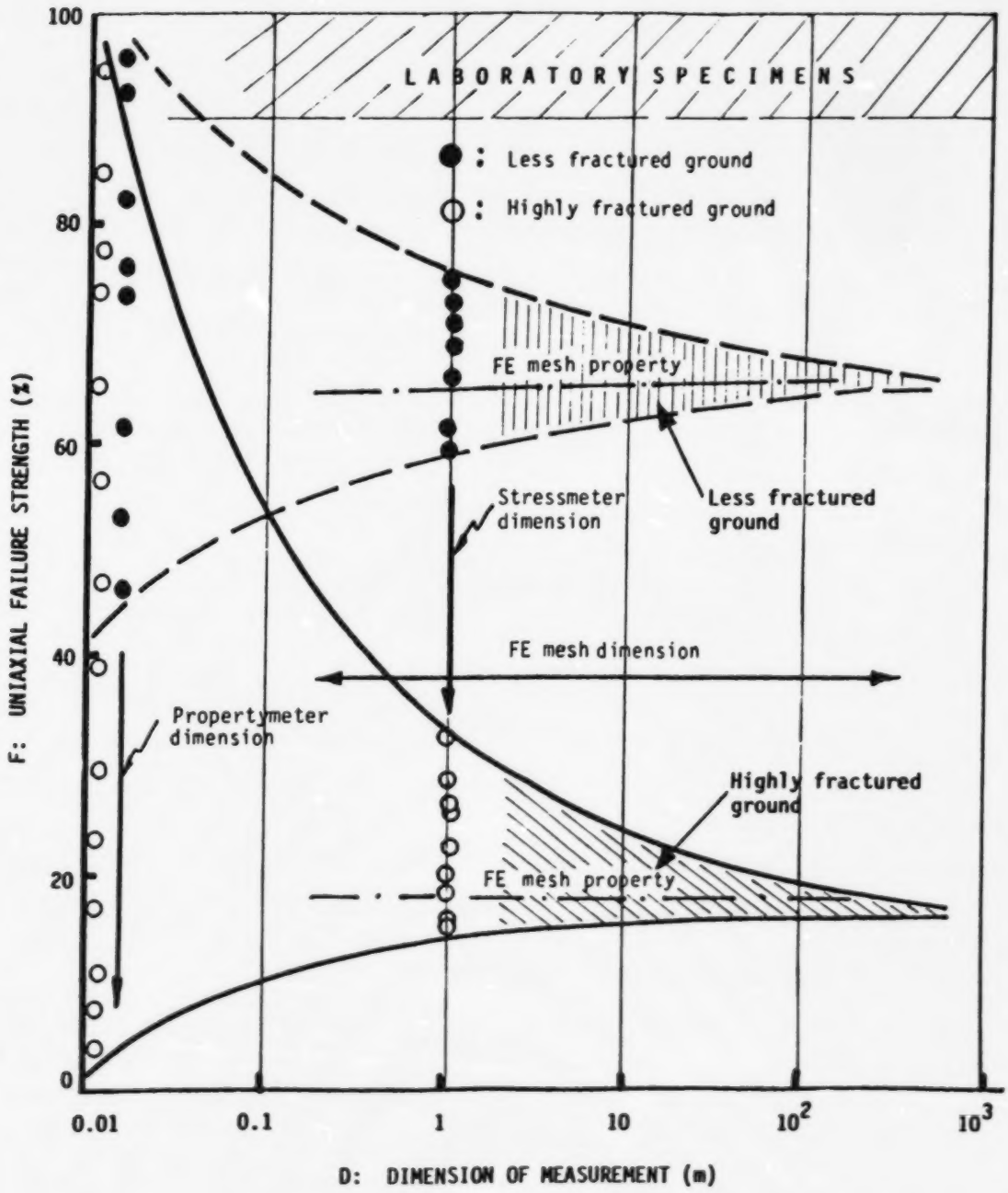

FIG. 3. Relationship among uniaxial failure strengths of prefractured rock media measured by three testing methods (S-200, P-200, and laboratory specimen testing) showing dimensional effect

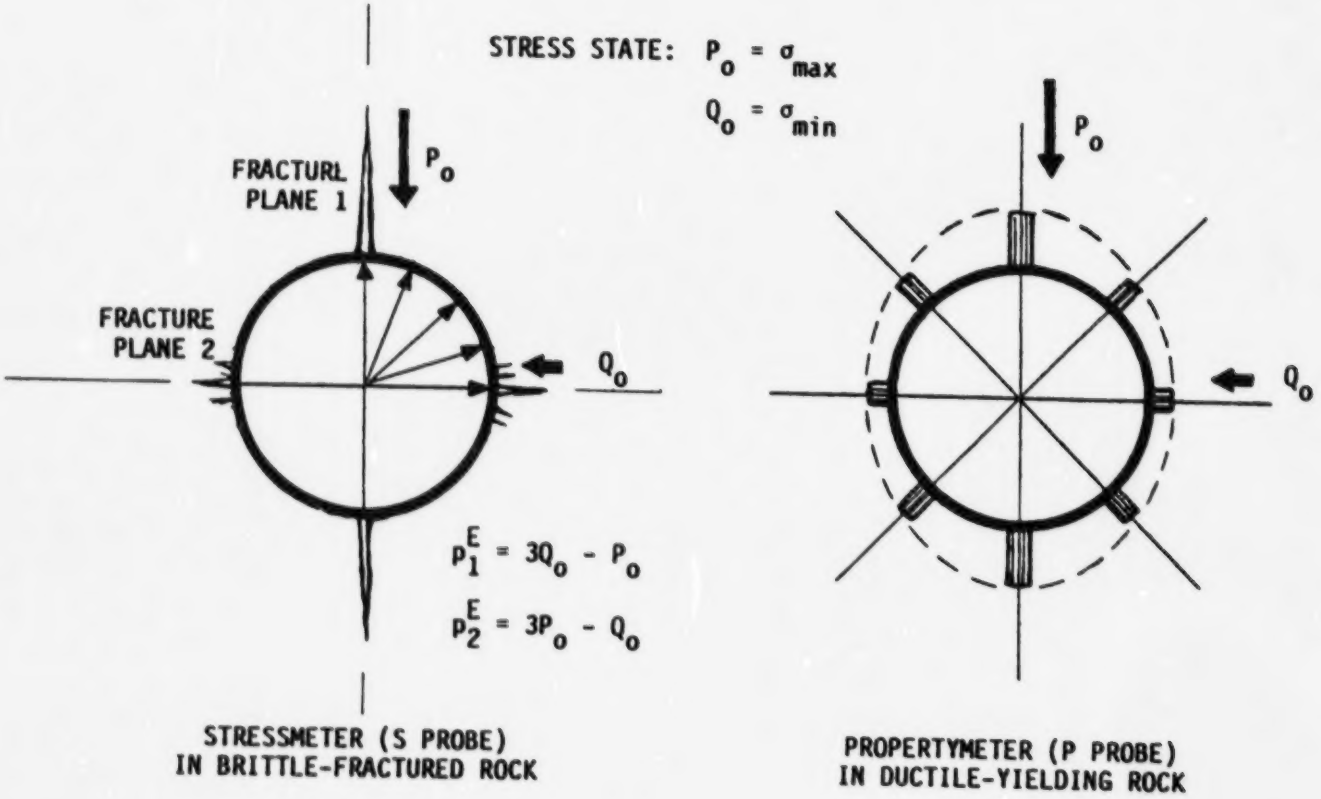

FIG. 4. Comparison of stress measurement configuration with S probe for brittle-fractured rock and P probe for ductile-yielding rock

respectively. The p_1^E and p_2^E values are detected from a characteristic change displayed in the diametral deformation pattern monitored directly by a set of eight LVDTs mounted inside the plastic loading cylinder. The orientation and magnitude of the maximum and minimum stresses (P_o and Q_o) are calculated from the pair of simultaneous equations noted in Fig. 4 [4]. Effects from microfractures are eliminated by the boundary media consolidation; effects from macrofractures are avoided by moving a slight distance from any measurement position producing anomalous readings.

In ductile-yielding rock, the S probe cannot create fracture planes because the borehole boundary starts yielding by shear before any tensile fracture can develop. As a result, the borehole diameter expands uniformly with no orientational difference regardless of different P_o and Q_o values. The uniform diametral expansion is directly related to the mean stress value of $\sigma_m = (P_o + Q_o)/2$. The P probe is applied in the same test borehole; its eight pistons penetrate into the borehole wall with the maximum and minimum penetration to the P_o and Q_o directions, respectively, disclosing the stress orientation, as shown in Fig. 4. The stress magnitude is determined by modeling the behavior of the S and P probes using the REM computer program developed for that purpose.

REM FINITE ELEMENT MODELING (R)

Finite element modeling of complex ground requires constitutive equations that can represent the stress-strain behaviors of all conceivable earth materials under widely varying boundary conditions. The equations must also represent the time-dependent processes of strength deterioration, failure, and postfailure deformation. SGI introduced a set of generalized rheological constitutive relations for this purpose, which are capable of representing earth materials ranging from air, high-pressure gas, water, mud, soil, sand, soft rock, fractured rock, concrete, intact rock, to metal. This is achieved by systematically selecting an appropriate set of material property coefficient values for use in the equations. The rheological scheme of Fig. 5 illustrates the relation among the behavioral

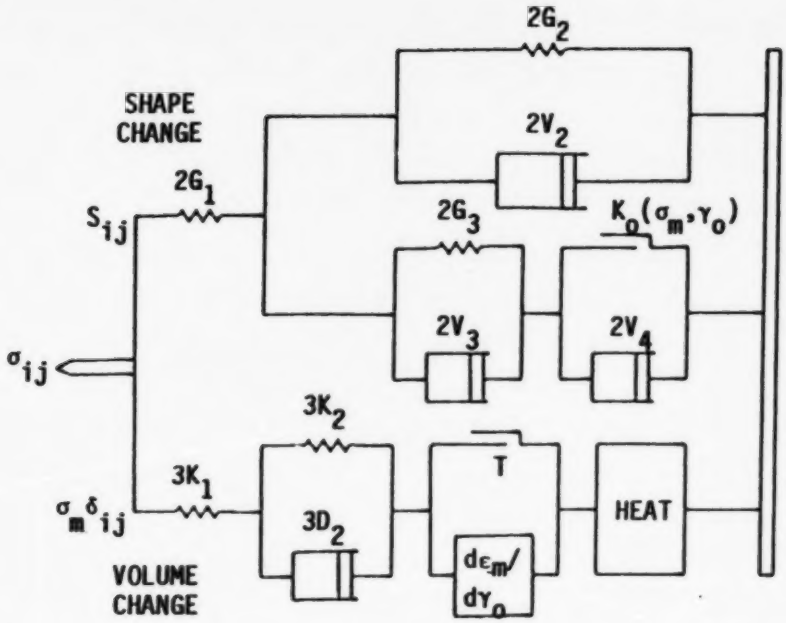

KEY

σ_{ij}: Stress tensor

ε_{ij}: Strain tensor

τ_o : Shear stress

γ_o : Shear strain

σ_m : Hydrostatic stress

ε_m : Hydrostatic strain

MATERIAL PROPERTY PARAMETERS

G_1: Shear modulus

G_2: Retarded shear modulus in viscoelastic state

G_3: Retarded shear modulus in viscoplastic state

V_2: Elastoviscosity in viscoelastic state

V_3: Elastoviscosity in viscoplastic state

V_4: Plastoviscosity in viscoplastic state

K_o: Octahedral shear strength

K_1: Bulk modulus

K_2: Retarded bulk modulus in viscoelastic state

D_2: Hydrostatic elastoviscosity in viscoelastic state

T : Tensile strength

FIG. 5. REM constitutive model of generalized earth materials

components of elasticity, viscoelasticity, viscoplasticity, yielding, thermal expansion, and failure. Further, the scheme represents the duality of material properties that causes the transition from brittle to ductile and vice versa according to the stress state. If necessary, any of the 11 fundamental coefficients defined in the figure can be expanded into a more elaborate function. Such separate functions are used to introduce the behaviors of strength deterioration, dilatancy, and postfailure deformation into the equation of Fig. 5.

SITE CHARACTERIZATION AND MODEL CALIBRATION

The SPDR Technology makes quantitative site characterization possible through numerical (FE) modeling of earthwork. As shown by the example in Fig. 6 of an underground opening in complex ground, the site-specific stress and property conditions are measured not only for the initial state but also for the disturbed state existing in the vicinity of the opening. As shown in the figure, the deviation of stress from its ideally elastic state discloses the true nature of the global properties, which respond to the excavation.

Through this site characterization process, model calibration is achieved following the procedure outlined in Fig. 7. Using the measured initial S and P values acquired in step 1, the REM computer model of the ground is constructed in step 2. The basic model thus developed is used to perform the design analysis in step 3. Results of the design analysis are applied in step 4 with the onset of earthwork construction, which provides the in situ testing site. The computer-simulated S and D around the test opening are measured in situ in step 5. The modeled and measured S and D conditions are compared and analyzed in step 6; the differences are then reduced or eliminated by modifying the P values through regression analysis in step 7. This causes the P values to approach the actual material properties of the ground without the necessity of knowing every fracture and anomaly in the formations. With the set of in situ P values thus established, the computer model is calibrated quantitatively and site-specifically in situ for practical application.

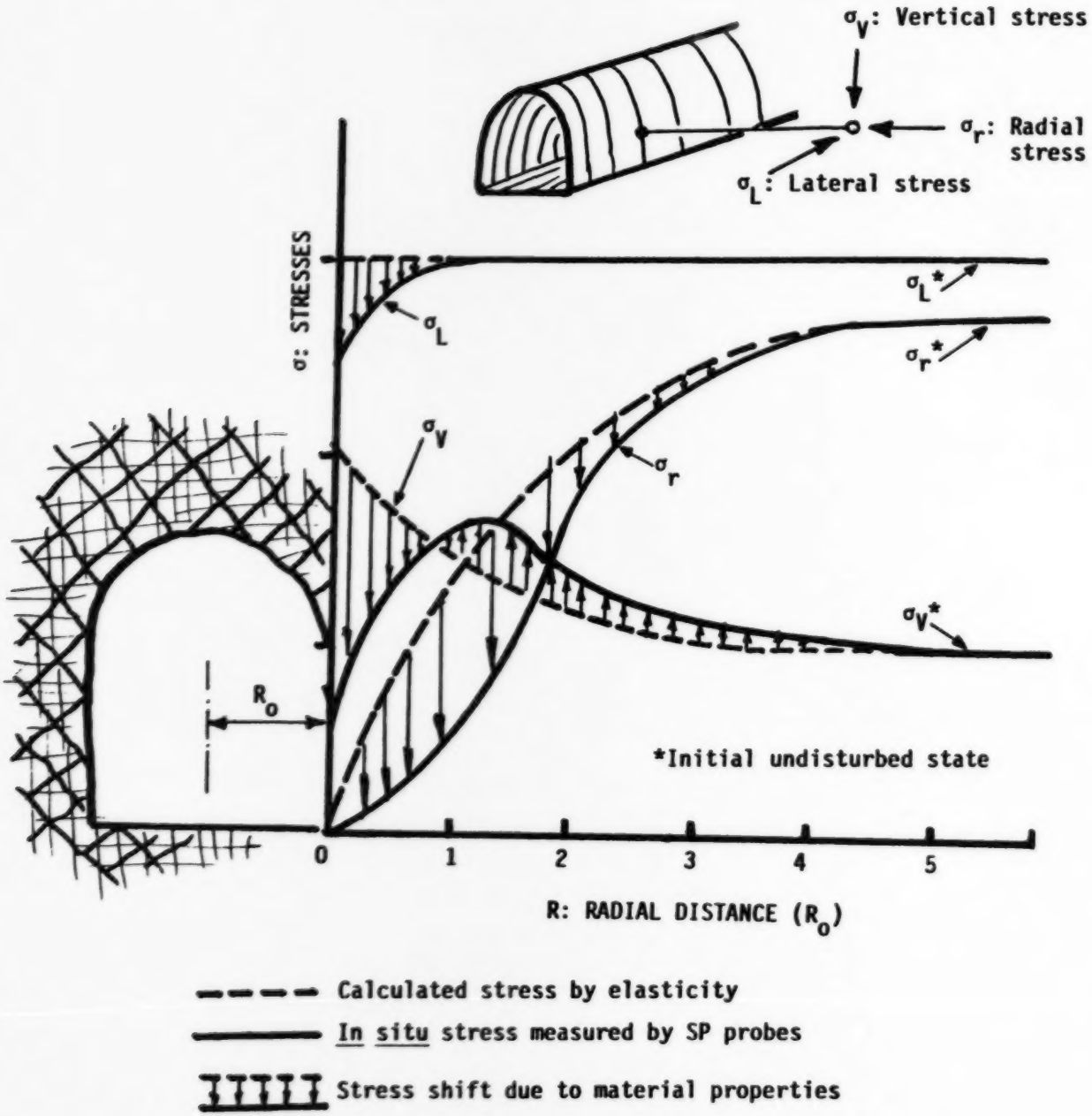

FIG. 6. In situ stress distribution pattern around excavation to be determined by SP measurement system, disclosing stress shift due to response of ground media to excavation

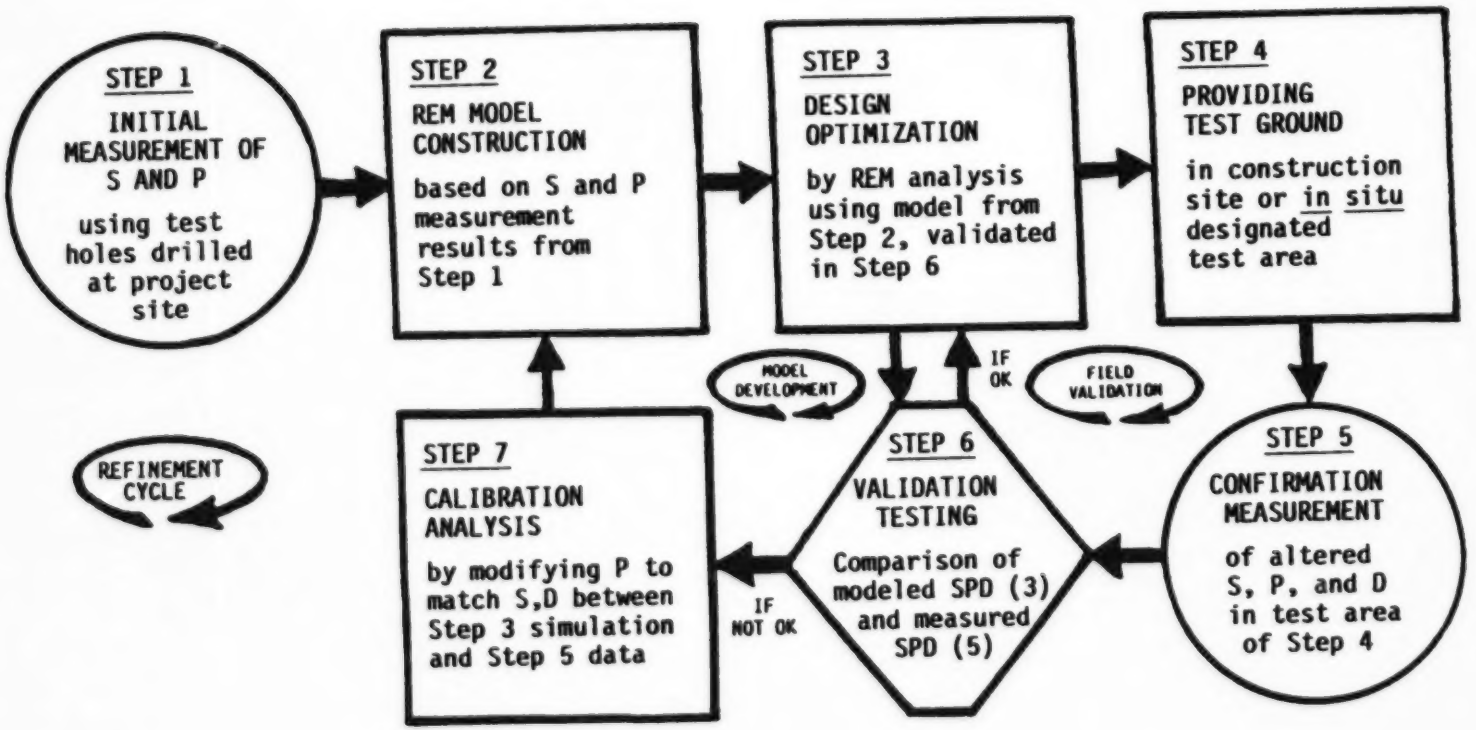
STEP 1
INITIAL MEASUREMENT OF S AND P
using test holes drilled at project site
STEP 2
REM MODEL CONSTRUCTION
based on S and P measurement results from Step 1
STEP 3
DESIGN OPTIMIZATION
by REM analysis using model from Step 2, validated in Step 6
STEP 4
PROVIDING TEST GROUND
in construction site or in situ designated test area
MODEL DEVELOPMENT
IF OK
FIELD VALIDATION
REFINEMENT CYCLE
STEP 7
CALIBRATION ANALYSIS
by modifying P to match S,D between Step 3 simulation and Step 5 data
STEP 6
VALIDATION TESTING
Comparison of modeled SPD (3) and measured SPD (5)
IF NOT OK
STEP 5
CONFIRMATION MEASUREMENT
of altered S, P, and D in test area of Step 4

FIG. 7. SPDR scheme of REM computer modeling of complex ground applied to planning, cost analysis, design, construction, and safety assessment of rock structures

CONCLUSIONS

The SPDR Technology is directly applicable to civil engineering projects, especially with regard to planning, cost estimating, design, construction, and safety analysis. A basic REM computer model is constructed using the initial stress state and property information obtained from SP testing in exploration boreholes. This model is utilized to make planning realistic and cost estimating quantitatively reliable. Candidate designs are explored using the site-specific model by conducting "what-if" analysis of the prospective construction. Construction management is enhanced by use of computer-predicted behaviors of S, P, and D as a reference to evaluate adequacy of the work. Finally, through the construction evaluation, the REM model is calibrated and applied for accurate assessment of the long-term safety of the earthwork.

The SPDR Technology enables rock mechanics studies to be performed on a scientific basis. The second article in this series will discuss in detail the hardware system used in making the S, P, and D measurements. The third and final article will present field examples showing the effectiveness of the technology in solving complex problems in rock mechanics work.

REFERENCES

1. Serata, S., 1982, "Stress Control Method: Quantitative approach to stabilizing mine openings in weak ground," in Proceedings, 1st International Conference on Stability in Underground Mining, Vancouver, 16-18 August.

2. Serata, S. and Lawshe, M., 1989, "Stress Control Method helps to optimize underground mine design," Mining Engineering, vol. 41, no. 3, pp. 158-160.

3. Kuesel, T.P., 1989, "An education in tunneling," Civil Engineering, March (pp. 76-78) and April (pp. 54-56).

4. Serata, S. and Kikuchi, S., 1986, "A diametral deformation method for in situ stress and rock property measurement," International Journal of Mining and Geological Engineering, vol. 4, pp. 15-38.

Appendix B

NUMERICAL RESULTS OF REM SIMULATION

Appendix B1 (Run 1)

Material property set: Norm

Slope geometry: $\alpha = 45^{\circ}$, $\beta = 57^{\circ}$

Timing of excavation: 3 months

Excavation sequence: Simultaneous removal of coal and overburden

Initial stress state: Hydrostatic (lithostatic)

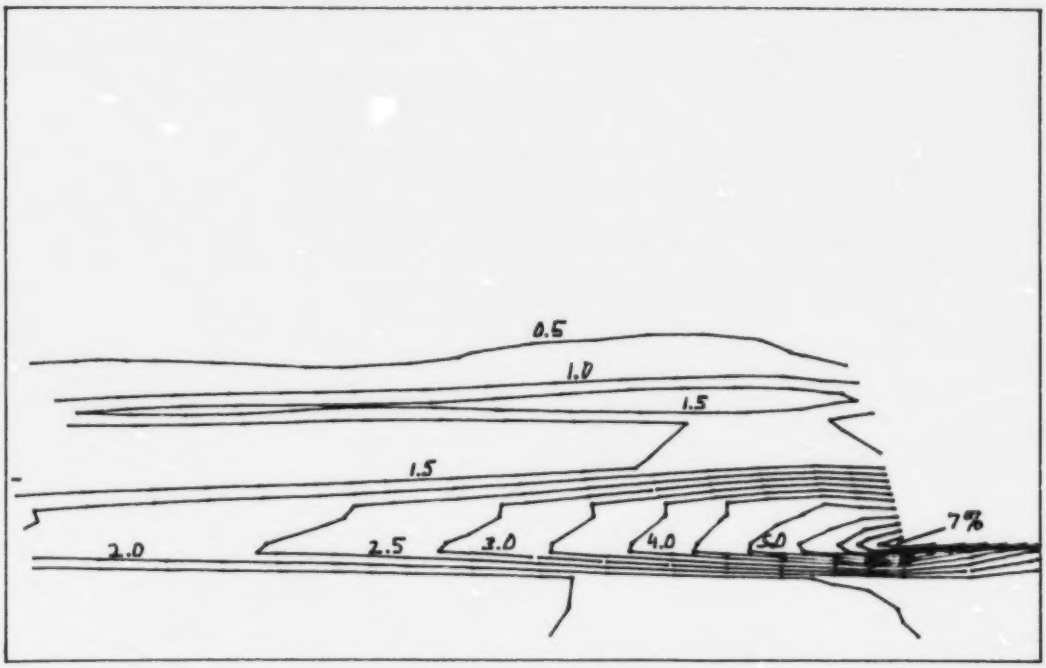

FIG. B1-1. Octahedral shear strain contour plot for final slope

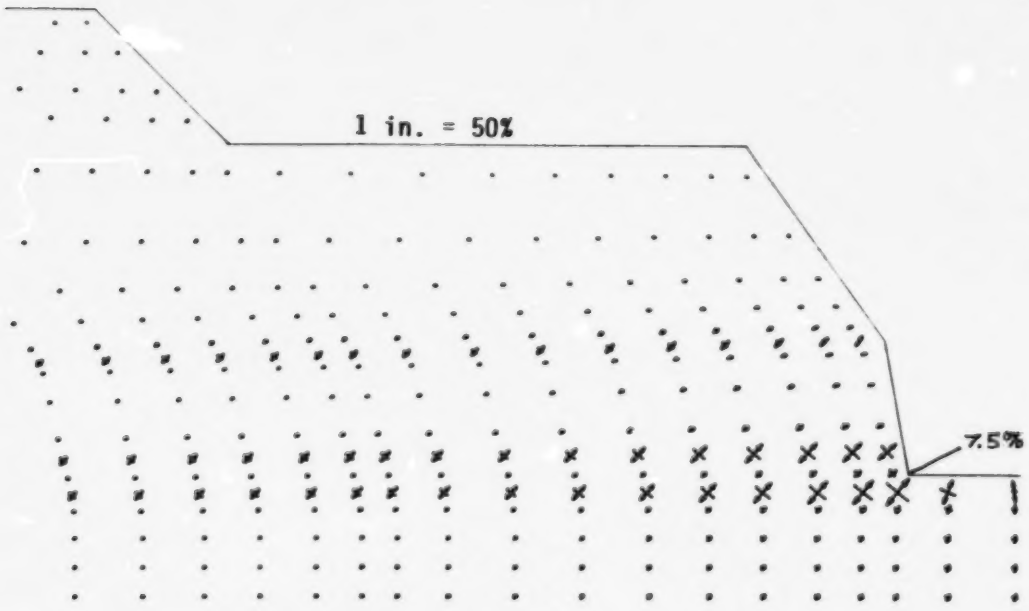

FIG. B1-2. Principal strain distribution around final slope

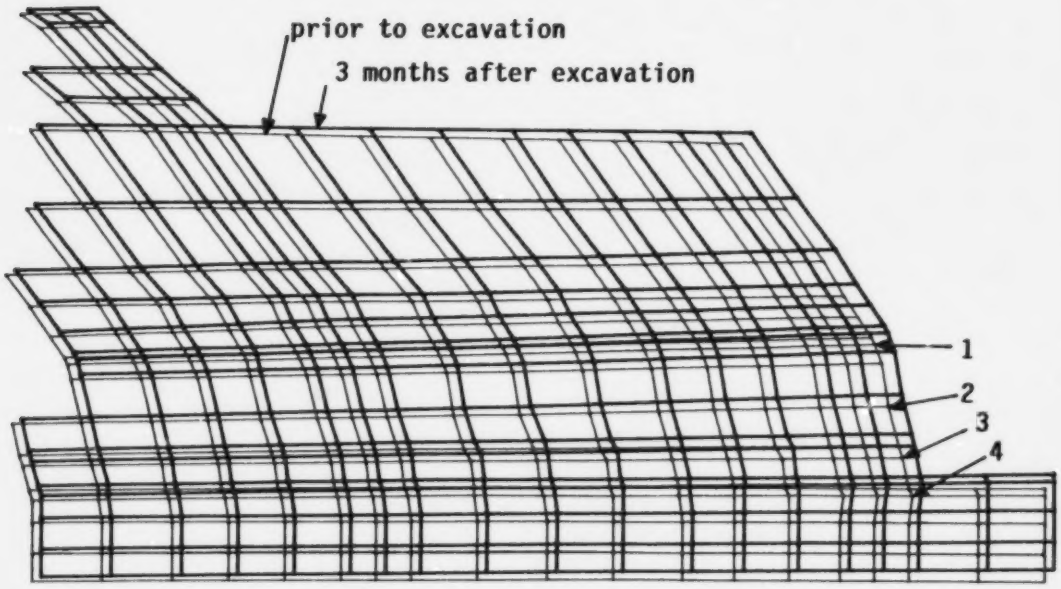

FIG. B1-3. Deformation of final slope

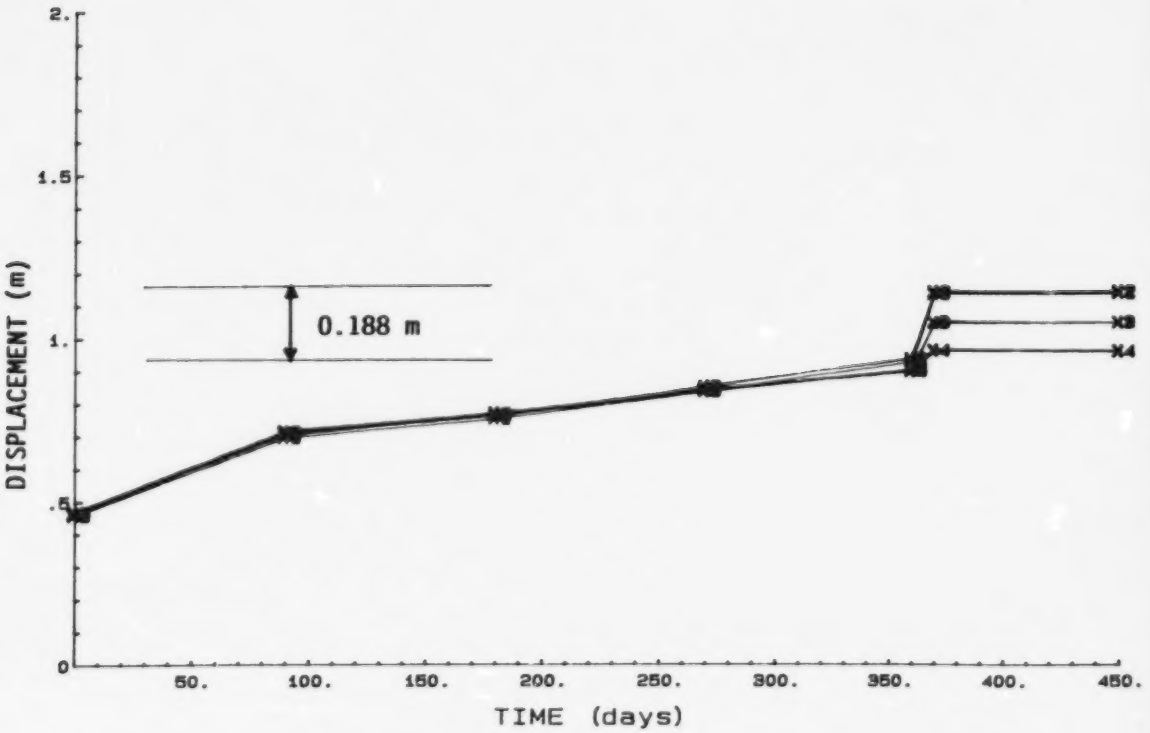

FIG. B1-4. Displacement of critical nodes in final slope

Appendix B2 (Run 2)

Material property set: Norm

Slope geometry: $\alpha = 50^{o}$, $\beta = 65^{o}$

Timing of excavation: 3 months

Excavation sequence: Simultaneous removal of coal and overburden

Initial stress state: Hydrostatic (lithostatic)

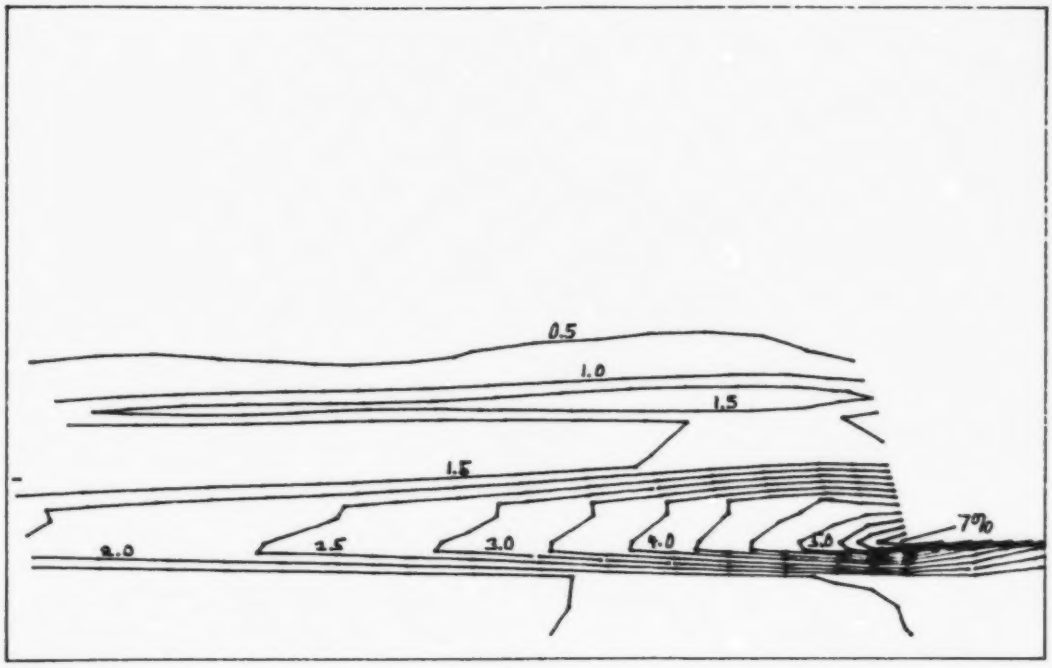

FIG. B2-1. Octahedral shear strain contour plot for final slope

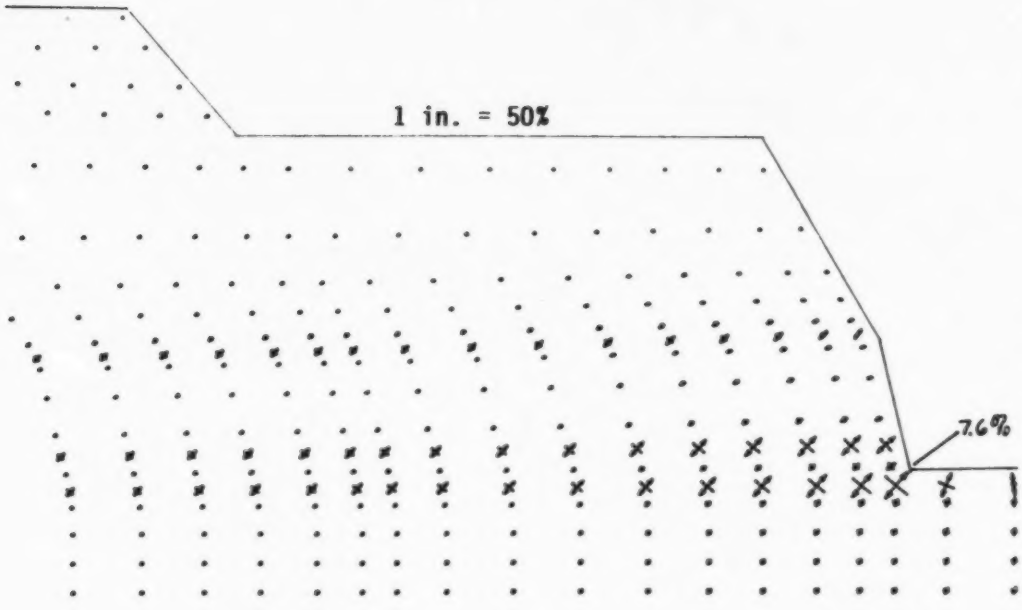

FIG. B2-2. Principal strain distribution around final slope

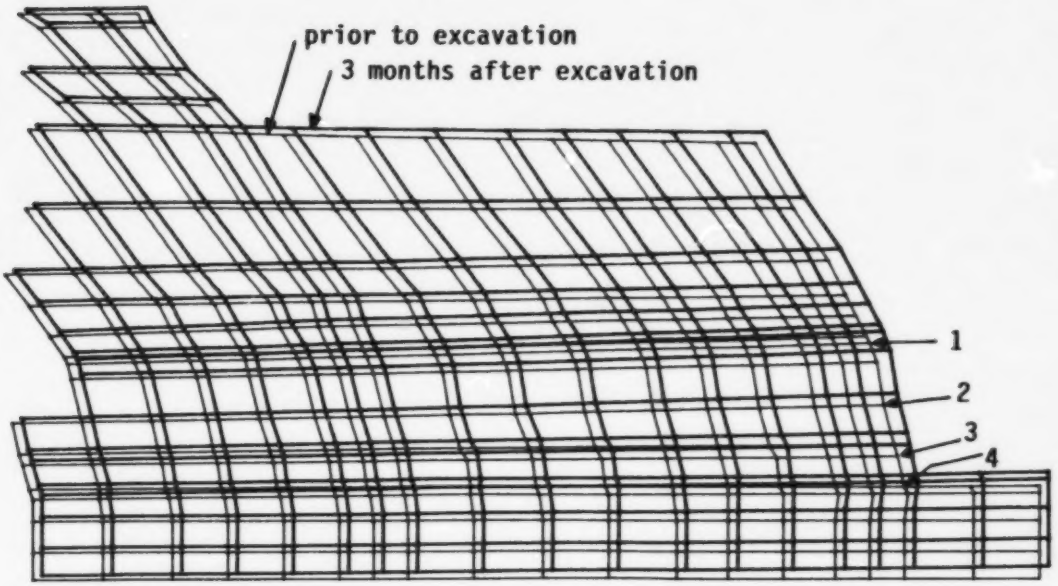

FIG. B2-3. Deformation of final slope

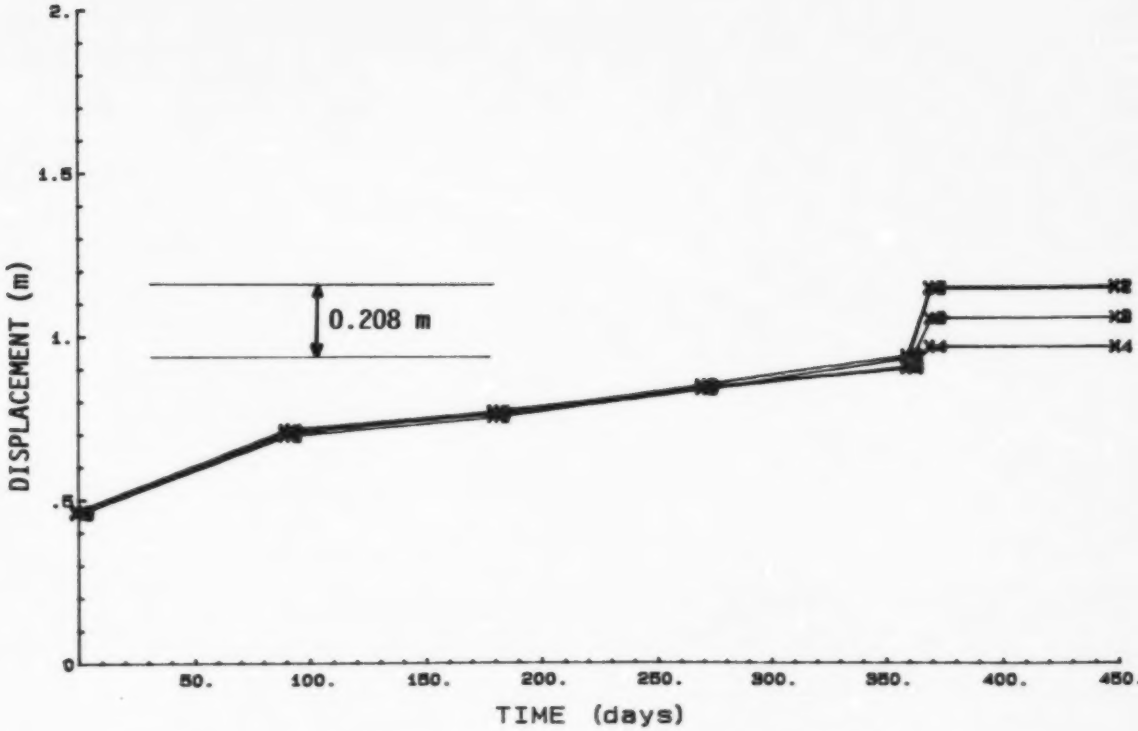

FIG. B2-4. Displacement of critical nodes in final slope

Appendix B3 (Run 3)

Material property set: Norm

Slope geometry: $\alpha = 55^{o}$, $\beta = 72^{o}$

Timing of excavation: 3 months

Excavation sequence: Simultaneous removal of coal and overburden

Initial stress state: Hydrostatic (lithostatic)

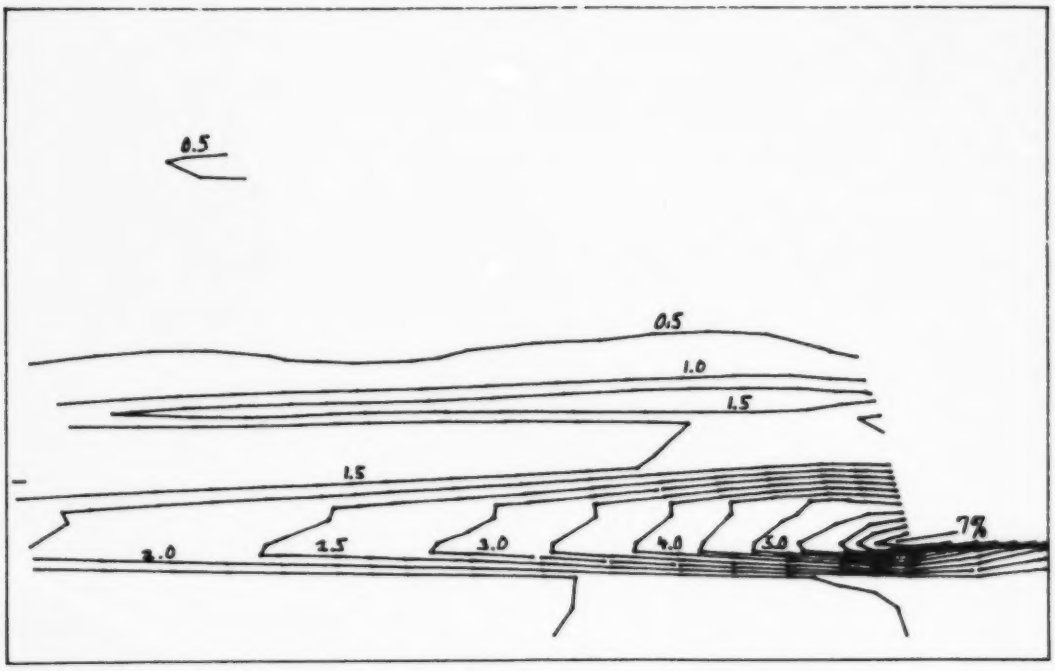

FIG. B3-1. Octahedral shear strain contour plot for final slope

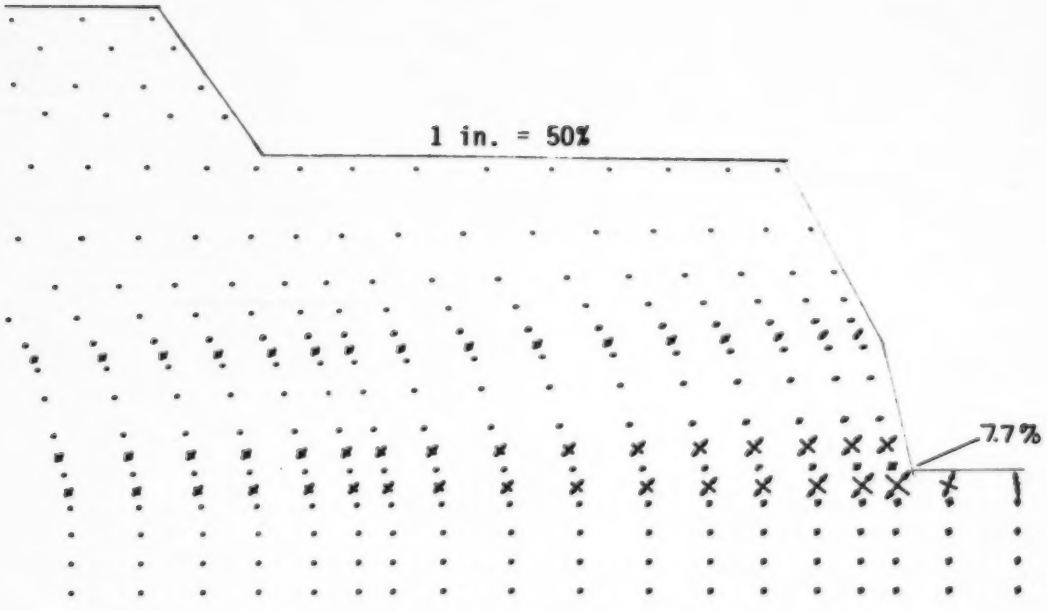

FIG. B3-2. Principal strain distribution around final slope

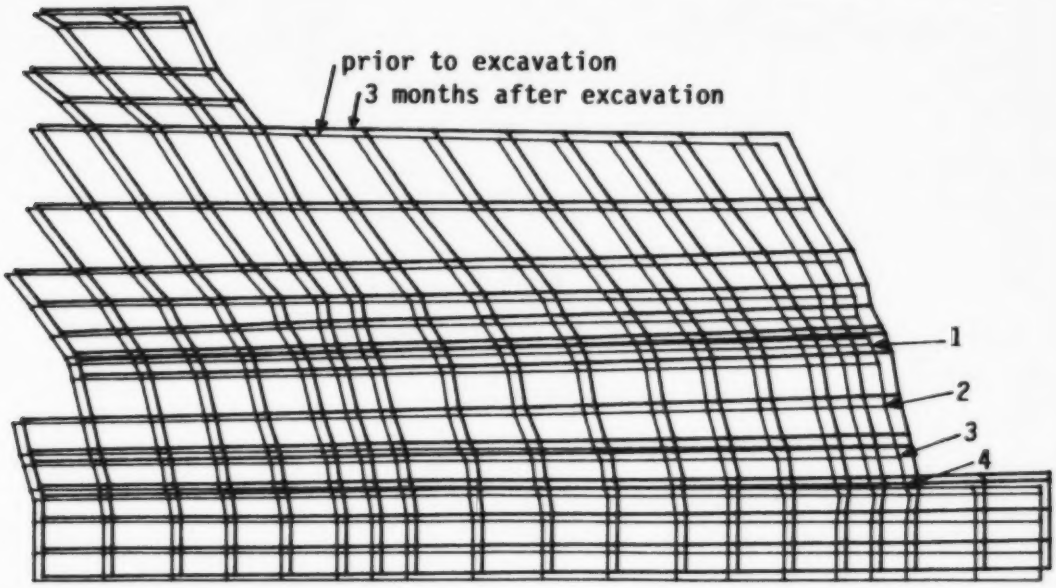

FIG. B3-3. Deformation of final slope

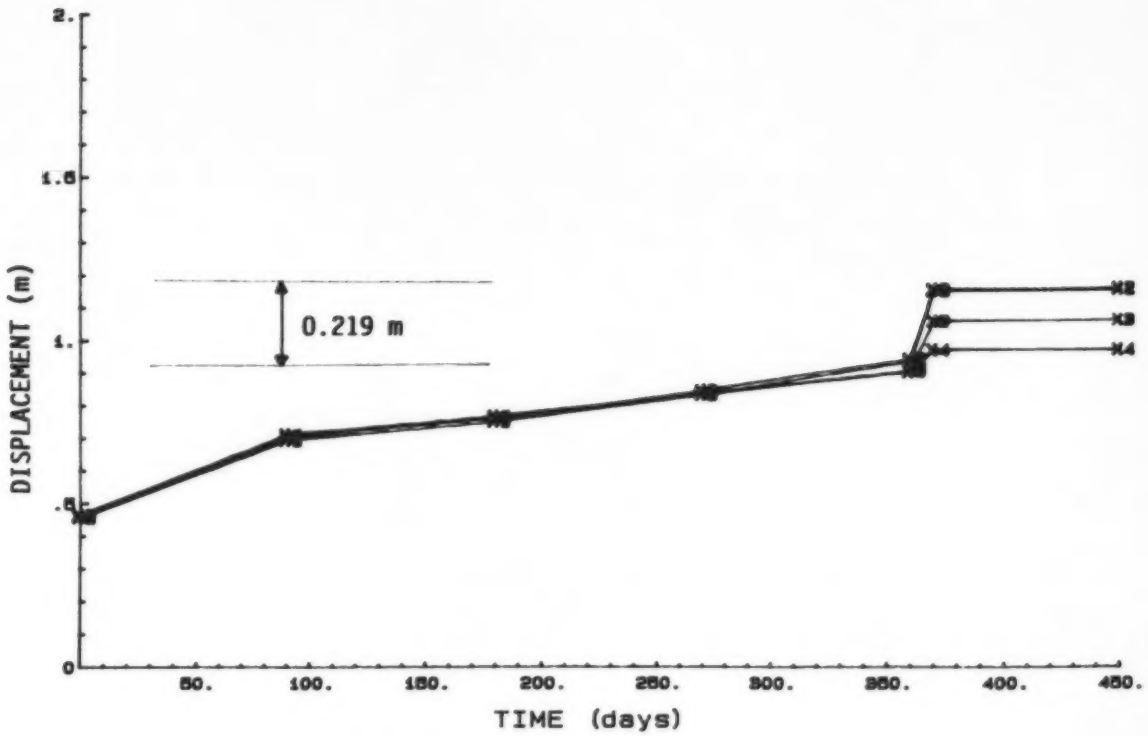

FIG. B3-4. Displacement of critical nodes in final slope